Physics – Uspekhi **63** (6) 562 – 582 (2020)

REVIEWS OF TOPICAL PROBLEMS PACS numbers: 95.75.Fg, **97.10. – q**, **97.82. – j**

Study of exoplanets by spectroscopic methods

V E Panchuk, Yu Yu Balega, V G Klochkova, M E Sachkov

DOI: https://doi.org/10.3367/UFNe.2019.07.038597

Contents

Abstract. A review of spectroscopic methods for observations of stars in searching for and studying exoplanets is presented. Instrumental errors in measuring radial velocities and strategies to decrease (or fundamentally eliminate) them are considered. The role of astrometric and photometric methods is pointed out. The results of the study of the chemical composition of parent stars and the spectroscopy of transit phenomena are discussed. Some promising directions are evaluated. The development of Russian ground-based and orbital instruments for spectroscopy and spectropolarimetry of stars is reported.

Keywords: extrasolar planets, stars, spectroscopy

1. Introduction

The number of publications on exoplanets (extrasolar planets) has been increasing sharply (according to the Astrophysics Data System: 7 publications in 1991–1995, 69 in 1996–2000, 742 in 2001–2005, 3497 in 2006–2010, and 13,905 in 2011–2018). The number of stars with planets found in their systems is somewhat smaller ($\sim$ 3900 were found by 2019). Therefore, reviews devoted to exoplanets are thematically limited. In this review, we focus attention on the technical aspect of the problem, which essentially determine the successes or failures of spectroscopic projects. The mention of selected theoretical papers here is only subsidiary and does not reflect our analyses in a field we do not work in.

The method of high-resolution spectroscopy is second in the efficiency of discovering exoplanets. The application of spectroscopic methods in the study of exoplanets can be divided into two areas: the search for new and the detailed investigation of already known exoplanets. In the first one, a decisive role belongs to mass Doppler measurements using specialized instruments with high accuracy maintained for a long time. In the second area, a key role is played by the limiting parameters of spectral instruments achieved today in the largest multiprogram telescopes. The epoch of discoveries and subsequent studies of exoplanets was preceded by a half-century of searching for them using photographic methods and photoelectric measurements with a small number of channels.

V E Panchuk [1,2,a], **Yu Yu Balega** [1,b], **V G Klochkova** [1,c], **M E Sachkov** [3,d]
[1] Special Astrophysical Observatory, Russian Academy of Sciences, 369167 Nizhniy Arkhyz, Zelenchukskiy region, Karachai-Cherkessian Republic, Russian Federation
[2] Space Research Institute, Russian Academy of Sciences, ul. Profsoyuznaya 84/32, 117997 Moscow, Russian Federation
[3] Institute of Astronomy, Russian Academy of Sciences, ul. Pyatnitskaya 48, str. 4, 119017 Moscow, Russian Federation
E-mail: [a] panchuk@ya.ru, [b] y.balega@presidium.ras.ru, [c] valentina.r11@yandex.ru, [d] msachkov@inasan.ru

Received 4 April 2019, revised 2 July 2019
Uspekhi Fizicheskikh Nauk **190** (6) 605 – 626 (2020)
Translated by M Sapozhnikov; edited by A M Semikhatov

2. Photographic methods: astrometry of nearest stars and Doppler spectroscopy

The presence of a small-mass satellite of a star can be detected from the features of its angular displacement (in the projection on the sky) and from changes in the line-of-sight velocity component (radial velocity). The accuracy of measuring radial velocity in estimating orbital parameters of a system with a small-mass satellite had long been inferior to the accuracy of determining the coordinates of a star. Therefore, the first indications of the existence of small-mass satellites of nearest stars were obtained based on astrometric

methods. The measurements of photographic images of the ξ Boo binary star obtained with a 61-cm refractor suggested the presence of a third body in the system [1]. Deviations from the orbit of the binary system were 0.02 arcseconds (semi-major axis) with a period of 2.5 years. The orbit projection on the plane of the sky was in fact a straight line, and therefore periodic variations of the radial velocity should be expected (within 4 km s^{-1}). The mass of the third component was estimated as 0.1 of the solar mass ($M_\odot$).

In the half a century of regular observations performed with the help of long-focus (focus distance $f > 10$ m) photographic refractors built in the late 19th–early 20th centuries, several systems with invisible components have been studied: Ross 614 [2], μ Dra [3], 61 Cyg [4], 70 Oph [5], and BD+5°1668 [6]. The highest measurement accuracy (probable error of 0.9 μm) was obtained [7] from observations performed by Kostinsky using a normal Pulkovo astrograph (image scale of 60 arcseconds per mm, $f = 3.5$ m). Papers [1, 7], in which the mass of the third component in the 61 Cyg system was estimated as $0.02M_\odot$ (20 Jupiter masses M_J), attracted the attention of Struve [8], who proposed a program of searching for extrasolar planets by measuring variations in radial velocities. Unlike astrometric methods suitable for studying about the 12 nearest stars, Doppler methods already at that time allowed fundamentally expanding the scope of searches.

The detection of small-mass satellites was not always confirmed by subsequent studies. By comparing photographic plates obtained in 1894, 1904, 1907, and 1916, Barnard [9] discovered a star with a record large proper motion (10.3 arcseconds per year). Later, van de Kamp [10, 11] analyzed 2413 photographic plates obtained in 1916–1962 and found oscillations of the trajectory of Barnard's star, which he explained by the presence of a small-mass satellite with the rotation period of 24 years (another satellite with a period of 12 years was added later). It was necessary to measure displacements of the center of the star image on photographic plates down to 0.001 mm. The search for a satellite of Barnard's star was performed using Fine Guidance Sensors (FGSs) of the Hubble Space Telescope (HST) [12]. Experimental conditions allowed the observation of a satellite whose mass exceeds Jupiter's ($M_J = 1.9 \times 10^{27}$ kg, which is 10^3 times smaller than the solar mass) with a period of more than 150 days. New constraints on satellite parameters were obtained after analyzing 248 measurements of the radial velocity [13] performed in 1987–2012 with coudé focus Hamilton spectrographs [14] of the 3-meter James Lick Telescope and the HIRES (High-Resolution Echelle Spectrometer) [15] of the 10-meter Keck Observatory Telescope.

We note that if the line of sight is perpendicular to the orbit plane of a hypothetical planetary system of Barnard's star, any variations in the star radial velocity should be absent. But a unique property of Barnard's star, in our opinion, is that among the four stars nearest to the Solar System, a representative of the ancient population of the Galaxy (about 10 billion years in age) is present. Some results obtained earlier by the method of photographic astrometry were confirmed by Doppler measurements (for ξ Boo [16] and BD+5°1668 [17]). So far, less than 1% of the total number of exoplanets have been found by modern astrometric methods [18].

The first reliable measurements of radial velocities were performed using spectrographs with photographic detection (Vogel, Belolpol'skii, Campbell, Adams). By the middle of the 20 century, more than 15,000 measurements of radial velocities have been performed with an accuracy of about 1 km s^{-1} (the mean accuracy was 750 m s^{-1}) [19]. It was assumed that such an accuracy was insufficient for detecting exoplanets (although later exoplanets were discovered with the half-amplitude of the radial velocity ~ 500 m s^{-1} [20]. It seems that here a stereotype played a role, which appeared based on the Solar System structure containing giant planets at large distances from the central star. Therefore, the search for Jupiter-like planets was believed to require the observation of a star for several years, maintaining the accuracy of measuring the radial velocity $\sigma(V) \sim 3$ m s^{-1} (if the line of sight lies in the planet orbit plane). In addition, it was assumed that planets should primarily be sought in systems with a central Sun-like star (the G5V spectral class).

By studying the distribution of the projection of the axial rotation velocity ($V \sin i$) on the line of sight for main-sequence stars (a drastic decrease in $V \sin i$ in passing through the F5 spectral subclass [21]), Struve proposed a hypothesis that cooler stars transformed the angular momentum of the axial rotation to the angular momentum of the orbital motion of planets. This leads to one of the first assumptions about the existence of numerous planetary systems. For this reason, Struve did not see arguments against the existence of a planet at a distance of 1/50 of an astronomic unit (AU) from the star. A hypothetical planet with the Jupiter mass M_J rotating at such a distance around a star with the solar mass $M_\odot$ with a velocity of 200 km s^{-1} and a period of one Earth day would produce Doppler shifts with the half-amplitude of 200 m s^{-1} (if the observer is in the orbit plane). A planet with a mass of $10M_J$ would produce radial velocity oscillations of ± 2 km s^{-1}. Struve also pointed out that for the average density of a giant planet exceeding the average density of the star by five times, the eclipsed fraction of the star disk area would be 1/50 and the radiance would decrease by 0.02 of stellar magnitude (which could already be measured by the first photoelectric photometers). The last conclusion opened up the possibility of detecting planets of fainter stars, which is impossible for photographic spectroscopy. It was proposed to start the program of searching for extrasolar giant planets with spectroscopic studies of broad binary systems for which the spectrum of one of the stars can be used as the reference spectrum [8].

We note that the average accuracy of 750 m s^{-1} in catalog [19] characterizes the variety of spectral instruments used in experiments and individual errors of a researcher rather than the accuracy inherent in each of the spectrographs. For example, the error of measuring the radial velocity from coudé spectra obtained with a 2.5-meter telescope was 23 m s^{-1} [22]. The coudé spectrograph of the 1.2-meter telescope at the Dominion Astrophysical Observatory (DAO) provides an intrinsic accuracy of 80 m s^{-1} and external accuracy (by radial velocity standards) of 200 m s^{-1} [23]. The intrinsic accuracy of these photographic observations allows the detection of an exoplanet with a mass of $0.005M_\odot$ in an orbit with the radius 2 AU. We note that the sensitivity of this spectrograph from a 1.2-meter telescope exceeds that of even the coudé spectrograph from a 5-meter telescope by more than one stellar magnitude [24]. Thus, it was the most efficient high-resolution spectrograph in the 1960–1970s. However, the accuracy of 100 m s^{-1} for photographic spectra was improved in [25, 26], where it was noted for the first time that a comparison of the absorption (stars) and emission (laboratory standard) spectra introduces

systematic errors into the calibration of the wavelength scale. As the reference spectrum, narrow molecular absorption lines in Earth's atmosphere (the so-called telluric lines) were used in [25, 26]. The reference spectrum and the spectrum of a star are formed for the same filling of the spectrograph aperture, and the influence of zonal errors distorting the point spread function (PSF) is then excluded [27]. Searches for small-mass satellites by the methods of photographic spectroscopy can be defined as the first stage of studies.

3. Instrumental errors of diffraction spectrographs

Errors in the determination of Doppler shifts are mainly instrumental and should be reduced in the ideal case to errors due to detector noise. However, this was attained only in rare cases, which are considered below. Errors inherent in known constructions are mainly instrumental [28] and, as a rule, are independent of the photodetector type. We consider the main errors and methods to eliminate them.

Earth's atmosphere works like a weak prism, which is manifested in the relative displacements of the centers of monochromatic images of a star on a slit [29], leading to relative shifts of spectral lines in different spectral ranges. The *atmospheric dispersion* effect can be partially compensated by placing a combination of prisms at the spectrograph entrance [30], which can be rearranged depending on the zenith distance. However, ideal compensation of the atmospheric dispersion in a broad spectral range is fundamentally impossible. The star image at the entrance slit of a spectrograph oscillates because of a set of intrinsic vibrational frequencies of the telescope construction and due to atmospheric turbulence.

The nonuniform illumination of the entrance slit causes displacements of the centers of gravity of monochromatic images of the slit. These displacements, averaged over the exposure time, vary from exposure to exposure [31]. The influence of the nonuniform illumination of the entrance slit can be considerably reduced by using a fiber-optic coupling of a telescope and a spectrograph and is in fact eliminated using an optical fiber with an aperture scrambler [32].

Experiments and estimates have shown that *the optical scheme instability* of a stationary mounted spectrograph is mainly caused by temperature variations in the parameters of the diffraction grating. Changes in temperature, pressure, and humidity affect the refractive index of air, thereby producing spectral line shifts. The influence of the instability of an optical construction and variations in the refractive index of air can be reduced by placing the spectrograph in a low-pressure volume with a thermostat [33–35]. In addition, if the simultaneous recording of the spectrum of a star and the reference spectrum is provided, the residual instabilities of the spectrograph are manifest in both spectra in the same way. If the stellar and reference spectra are formed with different contributions from different optical zones of the spectrograph, aberrations and zonal errors of optical units cause *a mismatch of the observation and reference channels* [27]. This effect can be eliminated by mounting an absorption cell at the spectrograph entrance [36–41]. In this case, the spectrum under study and the reference spectrum are formed both simultaneously and in the same aperture filling regime.

The star and reference spectra can be simultaneously recorded not only with the help of an absorption cell but also using a double-fiber spectrograph in which radiation from a reference source is delivered through the second fiber. While illumination by the reference spectrum is performed uniformly in time, the rate of illumination by the star spectrum depends on atmospheric conditions and the object tracking quality. Therefore, the average moments of the scientific and calibration exposures are different. This difference should be measured and taken into account in calculations of all Doppler corrections related to all motions of the observer point in the Solar System. For this purpose, the construction of a fiber-optic echelle spectrograph of the 1-meter telescope at the Special Astrophysical Observatory, Russian Academy of Sciences (SAO RAS) [42, 43] has an exposure control channel and an additional spectrograph for preparation of the reference spectrum.

Doppler shifts of a few thousand lines are mainly measured by cross-correlation methods, in which two circumstances should be taken into account. First, during cross-correlation processing, different spectral regions are not equal because of the variable density of the absorption distribution and image vignetting over the field of the spectrograph camera. Second, the use of field-flattening lenses and prisms as cross-dispersion elements, the presence of distortion, and, as a result, a change in the form of point diagrams over the spectrograph camera field complicate the measurement of the radial velocity by methods using spectral line shifts. The average linear spectral shift caused by the change in the radial velocity, which is constant on passing from one echelle order to another, is not constant within a given order [44]. In the red spectral range, it is necessary to exclude regions containing telluric spectral lines with different values of the radial velocity.

The disadvantages of algorithms for cleaning the traces of cosmic particles from images complicate the use of cross-correlation methods for a weak signal. When measuring radial velocities, it is desirable to have the line profiles in the star spectrum overestimated, i.e., to make the width of the resolution element in the spectrum smaller than the Doppler half-width. In this case, the error in the line shift measurement is proportional to the instrumental linewidth to the power 3/2 (see [45]). The full width at half-maximum (FWHM) of a weak line in the spectrum of a Sun-like star is about 0.07 Å at the wavelength $\lambda \sim 4500$ Å, and hence the region of efficient measurements of radial velocities for Sun-like stars begins with the spectral resolution $R = 130{,}000$. The spectral resolution is directly proportional to the diameter of a collimated beam and inversely proportional to the telescope diameter [46]. Therefore, achieving the spectral resolution $R > 60{,}000$ in large telescopes involves considerable losses of light at the spectrograph entrance (or losses in the number of simultaneously registered spectral elements if image slicers are used for light economy [47]). At the same time, observations with such values of R in moderate telescopes require such long exposures that the heliocentric correction of the radial velocity during these exposures considerably changes.

Passing from vacuum to semiconductor instruments did not completely justify expectations for improving the accuracy of positional measurements due to the use of solid-state detectors. CCD arrays demonstrate the influence of the nonrigidity of the photodetector unit on their operation [31, 48, 49]. The influence of the photodetector unit instability can be reduced by using repeated (or continuous) calibration. In the ideal case, the accuracy of measuring the radial velocity is restricted only by photodetector noise. This means that the influence of other systematic and random factors is consider-

ably reduced or excluded. Such examples of measuring radial velocities are already known [33, 50]. Below, we consider the features of different methods reducing or eliminating the influence of these errors.

4. Few-channel photoelectric methods

The measurement of individual positions of a few thousand absorption lines was a cumbersome and unattractive procedure, and therefore the introduction of correlation and digital correlation methods expanded the scope of researchers of radial velocities. In 1955, Fellgett [51] proposed a method for determining the average radial velocity not relying on measurements of positions of individual lines, but using the measurement of a signal transmitted through a movable mask of slits corresponding to spectral line positions. The first correlation photometer [52] was made already in 1966 and was used to measure radial velocities with an accuracy of 1 km s^{-1} for one photoelectric measurement. The advantages of a $D = 0.9$ m telescope operated only by one observation program (albeit for a poor image quality) were first demonstrated in a series of studies of spectroscopic binary systems by Griffin. To perform mass observations of radial velocities, several correlation photometers were built, which were used in coudé spectrographs operating in one spectral order of a diffraction grating [53–59].

The idea of a correlation mask was used in cross-dispersion spectrographs [44, 60, 61], and efficient specialized spectrographs appeared in [62–64], which were used with $D = 0.85 - 1.6$ m telescopes. These instruments provided an accuracy of 0.5–1.0 km s^{-1} on average and were considered inconvenient for searching for exoplanets. The CORAVEL (COrreation RAdial VELocity) spectrometer [62] mounted in the 1.5-meter European Southern Observatory (ESO) telescope provided an accuracy of 0.2 km s^{-1} for bright stars. Correlation photometers were used for the preliminary selection of stars. For example, in the program of searching for exoplanets at the Observatoire de Haute-Provence, the initial sampling consisted of 600 stars with radial velocities measured with CORAVEL with an accuracy of 0.3 km s^{-1}. The Doppler detection of a brown dwarf [65] showed that a single-channel correlation photometer allows the detection of radial velocity changes by 0.6 km s^{-1}, corresponding to the motion of a planet with a mass not smaller than $0.011 M_{\odot}$ (or $11 M_{J}$) in an orbit comparable to Mercury's. This result obtained from observations using an echelle spectrograph with a diode linear array mounted on a 1.5-meter telescope [66] was not considered to be detection of an exoplanet, because it gave a lower estimate of the mass (the orbit inclination remained unknown).

A breakthrough in the accuracy of photoelectric measurements occurred in the 1970s, when a spectrometer operating with a pair of photomultipliers or a linear diode array was built to search for exoplanets [67–71]. A drastic increase in the accuracy (to 10 m s^{-1}) was achieved by using a Fabry–Pérot interferometer (FPI) mounted in a vacuum chamber at the entrance to the echelle spectrometer. Spectra were scanned by changing the slope of FPI plates. We note that in the Serkovsky method, Doppler shifts were determined for the first time by measuring radiation fluxes transmitted in separate FPI orders (channels) rather than spectral line shifts.

In 1978, Connes proposed using an optical fiber in a correlation photometer [51, 52] and an FPI instrumental function (Airy function) instead of a mask. However, no financial support for the instrument construction was found, while astronomers who preferred 'classical' spectroscopy objected to the corresponding work on the coudé spectrograph at the Observatoire de Haute-Provence (see [72]). Connes's idea was realized by the amateur astronomer (a professional nuclear physicist) Flint [73], who built a private observatory. An autocollimation echelle spectrometer coupled with a 67 cm telescope by an optical fiber was equipped with an electrooptic FPI polarization modulator. Measurements in two polarizations were performed using two photomultipliers. Scientific results obtained with this instrument are unknown. Unfortunately, highly technological methods of applications of FPIs in Doppler measurements have not become part of mass methods so far.

Instrumental effects inherent in diffraction spectrographs are absent in the method using resonance cells with alkali metal vapors [74–76]. A sodium cell [77] placed into a magnetic field in combination with a linear polaroid mounted in front of it provides absorption in narrow spectral windows corresponding to the positions of Zeeman components of the resonance sodium line. The magnetic field strength is adjusted to tune spectral windows to the region of maximal steepness of the sodium line profile formed in the stellar atmosphere. The width of spectral windows is determined by the cell temperature. Radiation in the region of the sodium resonance line is separated at the instrument entrance by a narrow interference filter ($\Delta\lambda = 4$ Å). Two photomultipliers equipped with circular polarization analyzers detect resonance scattering components whose intensity is proportional to radiation entering the cell in the line wings. Another scheme [78] uses one photomultiplier, and polarization is switched with an electrooptic modulator. Here, the main source of errors (up to 1 m s^{-1}) is changes in the angle of radiation incidence on the modulator, i.e., guiding errors.

The main advantage of a resonance spectrometer is the high throughput (the instrument does not have a slit); the main disadvantage is the operation on one line, more exactly, on narrow fragments of the line profile. A fundamentally important circumstance is the stability of the wavelength scale, which makes the measurement of the *absolute* radial velocity possible. This method was used to detect and study five-minute oscillations of the solar photosphere. Both resonance spectrometers demonstrated the high sensitivity to the image position and azimuth of the Sun. Another advantage of the method is that resonance cells are *zero references*, because the properties of the same atoms (in the solar atmosphere and the instrument) are being compared. To study oscillations of the radial velocity, the system should be calibrated over all known motions, mainly Earth's motions. In this sense, the procedure is the same as in magnetograph observations: it is necessary to measure the day trend of the radial velocity each day and eliminate it. The remaining velocity oscillations are solar and of a helioseismic origin. This technique was also used for observations of bright stars. Fossat et al. [79] used a sodium cell in the absorption variant (where the quantum efficiency is higher than in the case of a resonance cell). For two nights of signal accumulation in a 3.6-meter telescope, the oscillations (p-modes) of α Centauri (stellar magnitude $m = -0.1$) were discovered. A disadvantage of the method is operation on one line near the absorption line center, where the radiation flux is minimal.

In [80], a pair of filters with bandwidths < 0.1 Å were used with their centers located symmetrically at the wings of the

NaI absorption line. A change in the relative velocity of the star–observer system causes changes in the radiation fluxes in filters. A magnetooptical filter is a cell filled with sodium vapors placed between two crossed polarizers in a longitudinal magnetic field. The cell blocks all the spectrum of a star, transmitting only wavelengths at which the magnetooptical effect is observed in sodium atoms. It was possible to observe single-mode oscillations with an amplitude of $50\,\mathrm{cm\,s^{-1}}$ (!) from a star with $m = 0$ with a 4-meter telescope for a night. This two-channel method also provided the helioseismic accuracy.

Asteroseismology methods, which allow reconstructing the density distribution over the star radius, have an accuracy sufficient for studying Earth-type exoplanets. Doppler measurements with instruments with few photoelectric channels can be defined as the second stage of searching exoplanets. This stage is characterized by complicated experiments and a variety of technological ideas and processing procedures.

5. Observations with multichannel spectrographs. First detections of exoplanets

Multichannel detectors with a high quantum efficiency were first introduced to classical diffraction spectrographs developed earlier for photographic detection. Reticon silicon photodiode linear arrays [81] combined in modules of up to eight arrays, a so-called Octicon, were used [82]. The detected spectral range was small, the accuracy of measuring Doppler shifts being determined by a small number of measured lines in the star and calibration spectra. Preferable were calibration methods free from zonal errors of the spectrograph optical units with the use of the telluric spectrum or a spectrum formed in the absorption cell. The presence of lines of the reference spectrum determined the operation wavelength range. The position and shape of the telluric spectrum lines depend on conditions in Earth's atmosphere, whereas the gas pressure and temperature in the absorption cell mounted at the spectrograph entrance can be maintained with a high accuracy. Absorption cells were filled with nitrogen dioxide (N_2O_4) for the wavelength range 3980–4600 Å [70], hydrogen fluoride (HF) for the wavelength range 8670–8770 Å [36, 37], and molecular iodine (I_2) for the range 5000–6000 Å. The last was first used in solar spectroscopy [83] and then in stellar spectroscopy [38, 84–86].

The accuracy of about $10\,\mathrm{m\,s^{-1}}$ maintained at a short time scale was sufficient for asteroseismology (study of the density distribution over the star radius [87, 88]), in programs involving the search for small-amplitude pulsations of cool stars [89–91], and in those studying the velocity gradient in atmospheres of Cepheids [92, 93]. It remained necessary to increase the number of simultaneously detected spectral lines and solve the problem of stabilization of spectrograph characteristics at the time scale of 1 year or more. One of the first long-term programs for searching for exoplanets was started in 1980 with the 3.9-meter Canada–France–Hawaii Telescope (CFHT) [94]. From three to six pairs of nights were allotted per year to this program for 12 years. Of course, because of a high duty cycle of observations, the probability of discovering short periodic changes in the radial velocity was low. Due to a small number of spectral lines used in experiments (in the spectral range ~ 100 Å, eight HF lines were used as references), the Doppler accuracy by one spectrogram was $15\,\mathrm{m\,s^{-1}}$.

The authors of [95] reported the probable discovery of small-mass satellites of two stars from 12 dwarfs and 4 subgiants observed for six years. The Lick observatory, where the second largest telescope with a 3-meter mirror was mounted in 1959, proved to be in the region of urban illumination of the night sky 20 years later. Because of this, the accent in observation programs gradually shifted to the spectroscopy of bright stars. In 1986, a cross-dispersion spectrograph with a CCD array was put into operation in the 3-meter telescope [14]. Mounted permanently in the coudé focus, the spectrograph operated each clear night with 3-meter or 0.6-meter telescopes, which increased the probability of discovering short periodic changes in the radial velocity.

In 1987, a program of searching for exoplanets was also started with a coudé spectrograph with the 2.7-meter telescope at the McDonald Observatory [96]. At the entrance to the California and Texas spectrographs, absorption cells with molecular iodine vapors were mounted. Astronomers at the Licks Observatory, who had lost some time on the reconstruction of the spectrograph camera, were closer to the discovery of exoplanets. The program of Doppler searches for exoplanets started on the FLODIE spectrograph [97] of the 1.93-meter OHP telescope in 1994 and encompassing 324 dwarfs of class G (brighter than stars with $m = 7.65$) provided a positive result already in 1995.

Mayor and Queloz [98] were the first to report the discovery of a small-mass dark satellite of the 51 Pegasi star. The FLODIE spectrograph was coupled to the telescope by two optical fibers, the second one delivering radiation from a hollow-cathode lamp to the spectrograph. To take the instability of the 51 Peg stellar atmosphere into account, additional high-precision photometric observations of the star were performed, and the stability of the correlation function form reflecting the expected line asymmetry was carefully studied. The stellar atmosphere proved to be stable [99].

The priority of the discovery was affected by some confusion in the spectral classification of 51 Peg. In the third edition of the Bright Star Catalogue (BS) [100], the 51 Peg star was classified as G5V, casting doubt on its photometric variability, while in the BS edition in 1982, the 51 Peg star was already classified as a G2.5IVa subgiant. Based on this classification, the 51 Peg star was excluded from the Lick program, which had begun in 1986, when it was reduced. After the discovery of the exoplanet, the 51 Peg star was again classified as belonging to the main sequence G2–G3V. During the subsequent 20 years, both methods of Doppler measurements (observations with an absorption cell and a fiber-fed commutation of a spectrograph with a telescope) were popular. Besides the OHR and Lick Observatory, several groups efficiently worked in Arizona [101, 102], Texas [103], and Hawaii [104]. Observation programs included from 20 to 140 stars and were intended for periods of 3 to 12 years. Therefore, the discovery of short periodic Doppler variations proved to be absolutely unexpected.

The history of the discovery of the first massive exoplanets was described in [105–107]. Here, we consider technological features of spectroscopy providing a high accuracy ($\sim 10\,\mathrm{m\,s^{-1}}$) of Doppler measurements. First of all, we note the role of multichannel photoelectric methods. Only after the introduction of photon-counting linear arrays was a brown dwarf discovered by the Doppler method [65], and the first exo-jupiters were discovered only using cross-dispersion spectrographs with CCD arrays [98, 108–113].

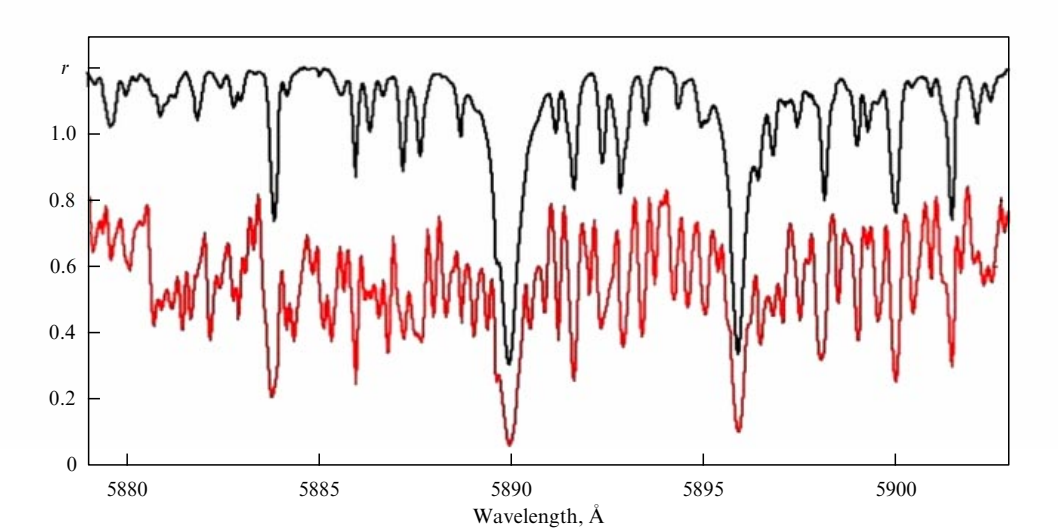

Figure 1. Parts of the one-order echelle spectra of a solar-type star obtained with the BTA. The upper curve is the stellar spectrum, the lower curve is the spectrum of the star and molecular iodine (displaced in the residual intensity r by 0.2).

The second factor is the choice of the most informative wavelength range, which already was made in the epoch of single-channel correlation photometers [114]. We note that in passing to the region of low-mass stars (cool M dwarfs), the red and near-IR spectral ranges (6000–9000 Å) become optimal (in flux and the number of lines).

The third factor is the spectral resolution $R = \lambda/\Delta\lambda$. As R increases, line overestimation occurs (when the width $\delta\lambda$ of the instrumental function of the spectrograph becomes smaller than the Doppler width of the spectral line) and the dependence of the Doppler accuracy on the line parameters changes [116].

The fourth factor is the long-term stability of opto-mechanical parameters of the spectrograph.

And finally, much is determined by the calibration technique and digital processing of spectrograms. The use of an iodine cell eliminates the problem of mismatch of the star and calibration channels; the spectrograph optical elements are then filled with light collected from the star and transmitted through the cell. It is also important that the spectral lines under study and the reference spectral lines are absorption lines. A limitation stems from the size of the wavelength range where the absorption spectrum of iodine molecules is observed. The absorption cell method is used in both multiprogram and specialized telescopes [14, 15, 39–41, 117–121]. Figure 1 presents parts of a star spectrum and a star spectrum with iodine obtained with the Big Telescope Azimuthal (BTA) in the late 1990s (see also [40, 41]).

Searching for massive exoplanets with multiprogram telescopes can be defined as the third stage of studies. In these studies, planets with a mass of about Jupiter's mass were discovered in very low orbits (with radius $\leqslant 0.05$ AU). Good reasons appeared for refining the existing [122, 123] and developing new [124–127] concepts about the formation of planets in the Solar System and exoplanet systems. A bias for comparing them with planets of the Solar System remained: the exoplanets being discovered are distributed by the usual categories (jupiters, neptunes, earths) with the addition of 'hot', 'super', etc. The characteristic feature of the third stage became the interaction of spectroscopic methods with other methods of discovering and studying exoplanets ('nonspectroscopic' methods are briefly considered in Section 7).

The next stage involves the regular use of several instruments [3, 34, 48, 128–140] specialized to provide a high Doppler accuracy. As a result, the statistics of Doppler measurements increased and the role of observational selection effects was estimated. Observations were performed synchronously with observations of photometric effects that manifest themselves during the transit of a planet over the star disk.

6. Wavelength scale calibration problems

The accuracy of Doppler measurements presented in the literature is specific to each particular telescope/spectrograph combination. In comparing results obtained with different instruments, the features of calibration procedures of Doppler measurements must be taken into account. Errors introduced in comparing emission lines of the calibration spectrum with the absorption lines of the star spectrum were first pointed out already in [25, 26]. However, calibration by the emission spectrum of a lamp with a hollow cathode covered with thorium salts is still used, in particular, in spectrographs coupled by optical fibers with telescopes. In studies using absorption cells, an accuracy of ~ 10 m s^{-1} was achieved, while a model accounting for variations in the point spread function (PSF) over the camera field gave an accuracy of 3 m s^{-1} [141]. We note that to achieve such an accuracy, it was necessary to reduce the effective area of the telescope objective by 30%, which was achieved by placing corresponding masks into the collimated beam [39].

Calibration methods can be divided into two groups: a comparison of the absorption spectrum of a star with the emission spectrum of a laboratory source and a comparison of the absorption spectrum of a star with the absorption laboratory spectrum. The main method of the first group is the two-fiber one, in which the emission of a star is coupled to a stationary mounted spectrograph through a 'scientific' fiber, and the emission of a hollow-cathode lamp is coupled through a 'calibration' fiber. The closely spaced bands of the scientific and calibration spectra are detected by different elements of a photodetector. The instrumental errors appearing in this case can be eliminated by switching the functions of fibers [42]. The first group also includes the method of

formation of the 'emission' reference spectrum by transmitting a continuous spectrum though a Fabry–Pérot etalon [142] under stable conditions (in temperature and pressure). The peaks of the instrumental function of the etalon are distributed quasiuniformly over wavelengths, which reduces the errors in constructing the dispersion curve by the calibration spectrum. In the first group, an expensive 'laser comb' method [143–148] forming a system of equidistant bright spots of the same intensity is assumed to be the most accurate.

The advantage of second-group methods is the capability to simultaneously record scientific and calibration spectra by the same elements of the photodetector (the calibration spectrum overlaps the star spectrum), which eliminates instrumental errors appearing due to the different filling of the spectrograph optical elements by 'scientific' and 'calibration' light. The use of an iodine cell is limited by the range of the absorption spectrum of iodine (in addition, as temperature decreases, polymerization occurs on the optical windows of the cell). If a Fabry–Pérot etalon operating in reflection light is placed between the telescope and spectrograph, a system of equidistant absorption references is obtained on the star spectrum. In our opinion, this method is promising for a spectrograph [149] operating on the movable platform of the 6-meter BTA.

In 1983, Connes proposed a method of absolute astronomic accelerometry (AAA) [72]. The main advantage of this method is the transfer of Doppler measurements from the incoherent to coherent region, which fundamentally improves the accuracy. The idea of the AAA method appears to be based on the method of heterodyne spectroscopy [150] using the mixing of monochromatic frequencies in the optical range for measuring beat frequencies with the help of a conventional frequency meter. We note that the problems of stellar seismology were named as the primary application of the AAA method, while the search for extrasolar planets was secondary. The accuracy of measuring the velocity of the star center is restricted by a number of physical effects in stellar atmospheres (see [151–155]). Because of this, the gravitational redshift in the case of the Sun, equivalent to the Doppler shift of 600 m s^{-1}, can be determined only with an accuracy of ~ 100 m s^{-1}. On the other hand, *variations in the velocity* can be measured with an accuracy three orders of magnitude higher [77]. Based on restrictions known at that time from asteroseismological data, Connes formulated requirements for the AAA method according to which a stellar accelerometer should measure variations in the radial velocity with an accuracy of 1 m s^{-1} on the minute/hour scale (on which seismological effects were assumed insignificant for stars of most types). Such a high accuracy of acceleration measurements should be maintained for days, months, and years, depending on specifics of the exoplanet search problem. Thus, the principles of solar and stellar accelerometry were already developed in the early 1980s.

The transition to measurements of a coherent signal is illustrated in the scheme of a stellar accelerometer in Fig. 2. Radiation from the Sun as a star (i.e., collected from the visible hemisphere) or a part of the photosphere is delivered through an optical fiber to the entrance to a Fabry–Pérot etalon operating in the central spot. The spatial separation of the etalon orders is provided by an echelle spectrograph (Fig. 3) with the spectral resolution $R \sim 150{,}000$. The working surface of one of the plates of the etalon is covered by a layer of a transparent material ~ 100 Å in thickness. The

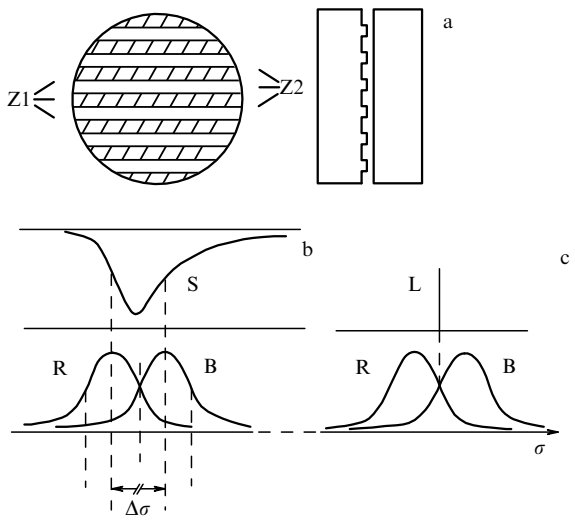

Figure 2. Operation principle of a solar accelerometer [72]. (a) Diagram of a double Fabry–Pérot interferometer (FPI); Z1: free zones of the FPI plate forming the long-wavelength (R) orders in a pair; Z2: deposited transparent layer strips forming short-wavelength (B) orders in a pair. (b) Positions and profiles of the orders of a double FPI with respect to the line profile S in the solar spectrum. (c) Positions of the L line of a tunable laser at the frequency scale σ.

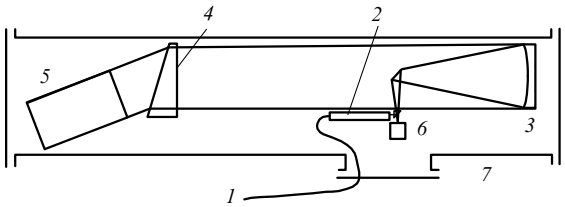

Figure 3. EMILIE echelle spectrograph [33] in the Littrow–Schmidt scheme: *1* — optical fiber with a diameter of 50 μm; *2* — matching optical elements; *3* — spherical mirror with a diameter of 305 μm, *f*/4; *4* — double-pass prism with an aspherical first surface; *5* — echelle-R2; *6* — CCD array; *7* — vacuum chamber.

layer was deposited through a mask in which the areas of deposited (Z2) and shadowed (Z1) zones are equal. Thus, one optical element combines two etalons, forming shifted systems of orders. The deposition thickness is chosen such that the same order of the etalon (with the number k_S) formed by zones Z2 and Z1 is shifted by a distance equal to the width of the line S in the solar spectrum being measured.

The difference $\Delta I_S = I_{RS} - I_{VS}$ between intensities measured at the wings of the solar-spectrum line by two detectors is used to form a signal controlling the thickness of the air gap between the etalon plates. The second signal comes from a tunable $\lambda = 6328$ Å He–Ne laser. The etalon Q-factor is chosen low to detect a monochromatic signal at each wavelength at two adjacent wings of the instrumental function of the etalon. Thus, laser radiation is detected in a pair of shifted orders with a different number (k_L) by a second pair of detectors. The intensity difference $\Delta I_L = I_{RL} - I_{VL}$ can be made zero by laser tuning. Therefore, the laser frequency can be used to monitor the tuning of the transmission bands of the etalon to the solar-spectrum line. By mixing the frequency of the tunable laser with the frequency of another laser, a stabilized one, beats can be obtained, which are then detected by a separate detector and

frequency meter. Thus, acceleration measurements are transferred from the field of incoherent radiation to the coherent field.

It was shown in [72] that the ratio N_{t1}/N_{t2} of beat frequencies obtained at two observation moments $t1$ and $t2$ is equal to the relative change in the radial velocity $(V_{t2}-V_{t1})/c$. The etalon thickness and the wavelength of the solar spectral line measured are excluded, and only the beat frequency has to be measured. The measurement error in a solar accelerometer limited by detector noise (with four channels at least: two for a solar spectral line and two for the laser line) proved to be three orders of magnitude lower than in the sodium cell method [77]. The stellar accelerometer differs from the solar one in that the radiation of the star under study should be treated parsimoniously. The absolute stellar accelerometer therefore uses information on the Doppler shift of many lines. A high-Q interferometer loses a considerable proportion of radiation in peaks of the instrumental function (see, e.g., [156, 157]). Therefore, Connes's stellar accelerometer does not use the transmission of stellar light through an FPI. Here, an important property of the solar accelerometer is used: a small detuning of the interferometer monitoring the Doppler shift is independent of the wavelength. The distribution of stellar spectral lines does not repeat the distribution of the transmission peaks of the interferometer, and hence the method of solar accelerometry cannot be extended to a large number of lines. However, *the Doppler shifts of the solar spectrum and the interferometer spectrum coincide*. The operation principle of the stellar accelerometer consists in the successive recording with the same multichannel spectrograph of radiation from a star and white light transmitted through the interferometer. As in the solar accelerometer, the state of the tunable interferometer is controlled by radiation from tunable and stabilized lasers, and the beat frequency is measured.

It is important that errors inherent in a diffraction spectrograph (listed above and in [28]) are excluded in an absolute stellar interferometer. For the quantum efficiency typical of CCD arrays in the early 1980s, the error of the acceleration measurement from the spectrum of a star with $m = 10$ with a 1-meter telescope for the 1 h accumulation time was estimated as 1 m s^{-1} [72]. The absolute stellar accelerometer was the first multichannel spectral instrument in which the accuracy of Doppler measurements limited only by the instrumental noise was achieved [50]. At present, the calibration accuracy of the best spectrographs is better than 1 m s^{-1} and can be maintained for several years. The central remaining question is whether the radial velocity of the star center (or the star–planet barycenter) can be reliably measured with the calibration accuracy by observing absorption spectra formed in the stellar atmosphere.

7. Combination of spectroscopic methods and other methods

According to the observation technique, the methods of detecting and studying exoplanets are divided into astrometric, photometric, and spectroscopic [158]. As mentioned, astrometric methods made a small contribution because they could be applied only to relatively close neighborhoods of the Solar System. New results are expected from studies with the PRIMA (Phase-Referenced Imaging and Microarcsecond Astrometry) interferometer of the VLT (Very Large Telescope) [159] and from orbital missions (see, e.g., [160]). Photometric methods are divided into transit methods (measurements of the parent star brightness during the transit of a planet over the star disk [8, 161–165] and methods of observing the reflection of star radiation from the planet disk [166]. The methods of exoplanet imaging using adaptive optics [167, 168] are more efficient in the IR region. The method of microlensing (rapid brightness variations observed during the transit [169, 170]) can be used to discover small-mass planets. However, the reliability of unrepeated microlensing effects can be confirmed only by simultaneous observations with the help of various instruments. A variant of photometric methods is measurements of deviations of the moments of transit events [171, 172], which can be used to discover additional gravitational perturbations in the system. Photometric studies of exoplanets also include direct observations using interferometers and coronagraphs of different types [173] but require an image contrast of the order of 10^{-10}. Coronagraph methods open up the possibility of spectroscopy of planet's atmospheres.

All the methods mentioned above detect a photometric signal identified in a broad spectral band. The Doppler method measures spectral line shifts caused by the rotation of a star around the star–planet barycenter. The oscillation period of the projection of the rotation velocity of the line of sight is related to the radius of the planet orbit. Because of the uncertainty in the orbit inclination angle i to the line of sight, only $M \sin i$ can be determined, where M is the planet mass. When photometric eclipses are also observed in the system, restrictions on the angle i become stringent, and the planet mass M can be determined. The mass and radius of the star can be estimated from the type of its spectrum, and the radius of the planet can be determined from the eclipse depth. If the planet size and mass are known, its density can be estimated. A combination of Doppler and photometric observations expands the statistics of exoplanet properties [175].

The development of transit photometry is manifested in spectroscopic observations. Observations with the HIRES (High Resolution Echelle Spectrometer) of the 10-meter Keck-I telescope gave the upper limit of the radiation flux reflected by the atmosphere of an exoplanet in the τ Boo system, which proved to be lower than 5×10^{-5} of the star flux [176]. In such experiments, it is necessary to construct a model of the star spectrum (based on the set of all the observed spectra, for example, 580 spectra in [177]) for separating the signal belonging to the planet from each observed spectrum. In this case, it is assumed that all the deviations of the observed spectrum from the model spectrum are determined by the spectrum reflected from the planet. If the planet orbit is known, the model spectrum can be constructed using the phases in which the contribution of reflected light is absent. The planet spectrum (in the case of τ Boo, reaching the maximum 10^{-4} of the stellar spectrum) separated for each phase by subtracting the model spectrum still 'sinks' in noise [178].

8. Restrictions on the accuracy of spectroscopic measurements of exoplanet parameters

We consider physical effects in atmospheres and envelopes that restrict the accuracy of measuring the radial velocity of the star center. In most cases, radiation entering a spectrograph is averaged over the star disk. The 'weight' of the

radiation flux coming from the central and periphery zones of the disk is well described by the theory of radiation transfer in a hydrostatic atmosphere. Motions in the stellar atmosphere also affect the spectrum, but the type of weight functions can be different (see, e.g., [179]). All this affects the determination of the velocity of motion of the star center.

Below, we list effects fundamentally limiting the accuracy of measuring radial velocities by methods in which the generalized information (averaged over the spectrum of a given star) on the shape and position of spectral lines is used. These methods include a variety of cross-correlation methods. The use of cross-correlation techniques assumes that the velocity field (radial gradient) in the stellar atmosphere does not change in time or variations in the gradient are insignificant at the scale of expected velocity variations.

The main phenomena that can decrease the accuracy are coherent oscillations, convective motions, supergranulation, stellar activity cycles, star outbursts, and axial rotation. To separate these effects from kinematic acceleration, it is necessary to construct an amplitude diagram of the velocity distribution. In the atmospheres of Sun-like stars, the amplitude of nonkinematic variations in the radial velocity integrated over the star disk is smaller than 100 m s^{-1}. Short-term variations (shorter than 1 h) related to coherent oscillations and supergranulation have small amplitudes for the Sun and have already been observed for bright Sun-like stars. Variations on the intermediate time scale (days to months) are caused by rotational modulation (when the line profiles are affected by large groups of long-lived spots or regions of outbursts).

The presence of active regions can modulate the cores of strong (chromosphere-sensitive) lines, while the shape and positions of weak lines are preserved. Therefore, in the Doppler search for invisible satellites of stars, with the major role played by weak and moderate-intensity lines, the influence of spots and active regions may be absent. Nevertheless, the position of strong lines should be verified against the correlation with emission in the K line of the CaII doublet (the modulation of these radiation fluxes by axial rotation is described in [180]). To perform simultaneous observations in the K line of CaII, a spectrograph operating in the spectral range optimal for Doppler measurements should be supplemented with a ground-based UV channel.

Figure 4 shows a part of the spectrum of the 16 Cyg A star, close in luminosity to the Sun. In this case, the features of the chromosphere activity can be observed only in observations with a high spectral resolution. Small-amplitude oscillations of the positions of absorption lines in the solar spectrum caused by variations in solar activity can be separated from all Doppler perturbations, which are well known for the Solar System.

In [182], solar spectra were obtained with the HARPS (High-Accuracy Radial velocity Planet Searcher) spectrograph [34] by observing light reflected from the Vesta asteroid during two axial Sun rotations, and non-Doppler line shifts equivalent to changes in the radial velocity by 15 m s^{-1} were separated. The HD 166435 star, known by its activity (photometric variations, emission in the H CaII line, variations in the shape of the absorption bisector) with a period about 3.8 days [183] was studied with the reconstructed ($R = 220{,}000$) CES (Coudé Echelle Spectrometer) spectrometer of the 3.6-meter ESO telescope [184]. It was shown that taking the line asymmetry due to the presence of cold spots into consideration reduced the variation amplitude of radial

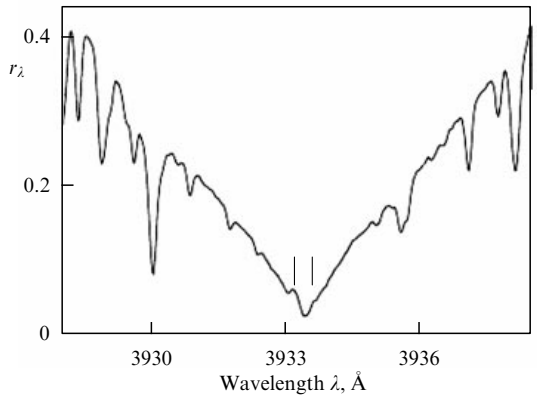

Figure 4. Central part of the K CaII line profile in the 16 Cyg A spectrum (G1.5Vb). Vertical bars indicate the remnants of the emission chromosphere profile: $\lambda = 3933.2$ Å K2v and $\lambda = 3933.6$ Å K2r (BTA observation presented in Fig. 1a in [181]).

velocities by one half. The active CoRoT-7 star was studied spectroscopically and photometrically in the absence of transits [185], with the data used to estimate the contribution of spots to photometry and convection to the shape of bisectors. In this case, non-Doppler variations of line positions were also determined.

The result of the search for long-period, small-amplitude oscillations of the radial velocity caused by the presence of an invisible component also depends on the line asymmetry due to photospheric granulation [151–155, 186]. The convective energy transfer in the stellar atmosphere is only a few percent of the radiative transfer. The radiation flux from the surface covered by convective elements (granules) is mainly determined by the hotter (bright) parts of convective elements. These parts ascend in the atmosphere and Doppler-line cores formed in them are blue-shifted. The cold parts of convective elements descending in the atmosphere cause a red shift of line cores. However, the contribution from cold parts is secondary because of the low brightness temperature. In the region of line wings, where the radiation flux is higher, the contribution from cold parts is somewhat higher than in the core. As a whole, the integrated line profile exhibits weak asymmetry (a blue-shifted line core).

The asymmetry effect is usually described by line bisectors — curves formed by a set of points equidistant from the blue and red wings of lines at the specified levels of the residual intensity r (Fig. 5). Lines of different depths are formed predominantly at different densities and temperatures, and therefore the asymmetry effect should be different from line to line (or between groups of lines with close intensities). If convective elements are large and their number is small, the asymmetry effect also depends on time. In this case, the radial velocity of the star is no longer described by a single quantity, and therefore asymmetry effects impose fundamental restrictions on the accuracy of measuring radial velocities by cross-correlation methods.

The spectrum of the Sun showed that the profiles of weak but magnetic-field-sensitive spectral lines change with the solar activity cycle [188]: cyclic variations in the surface magnetic field affect the convection, resulting in a change in the asymmetry of line profiles. The line bisectors at the intermediate depths of profiles can change by 75 m s^{-1} within the period of solar activity. Variations in the asymmetry of solar lines were also suspected in [189], and later this effect

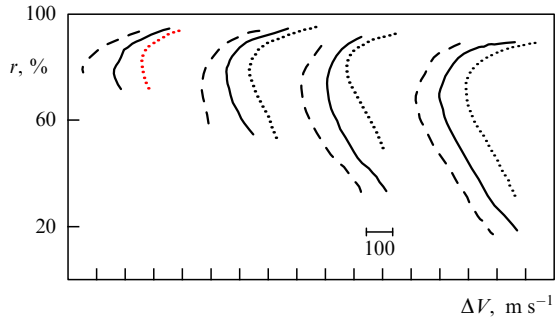

Figure 5. Mean bisectors for FeII line groups in the solar spectrum (Fig. 5 from [187). Solid curves: all lines; dashed curves: lines with a low excitation potential of the lower level, $0 < \chi < 3$ eV; dotted curves: lines with a high excitation potential of the lower level, $3 < \chi < 7$ eV. The lines are grouped by the value of the central residual intensity r; bisectors are moved apart in the velocity scale V. The abscissa scale division is 100 m s^{-1}.

was studied in detail in [190, 191] and simulated in [192, 193]. The HD 166435 star exhibits oscillations of the radial velocity with the half-amplitude 83 m s^{-1} and period 3.8 days [183]. Photometric observations and observations in the H and K CaII lines were respectively performed in order to search for the rotational modulation and signs of optical activity. It was found that variations in the radial velocity correlate with the orientation of bisectors of spectral lines, and photometric oscillations are shifted by a quarter of a cycle (about 30 days) with respect to variations in the radial velocity. This effect was observed for the two years of observations, and the HD 166435 star proved to be the most stable among active stars. A model of a magnetic rotator was proposed that explained the stable generation of spots by a magnetic field in the same region.

The stationary atmosphere of a star can be approximately described by a one-dimensional model based on the hydrostatic equilibrium equation. During star evolution, the energy release from different layers changes and the envelope and atmosphere begin to expand, which can be accompanied by the overflow of matter into the interstellar medium. When a certain amount of matter is lost, these processes are reflected in the shape of lines. For example, if there is enough matter in the expanding region formation of cores of strong lines, the radial velocities measured by the positions of the cores and wings of strong lines are different. If radial velocities are measured mainly by Doppler cores, such measurements can be systematically different for strong and weak lines. Because of this, the program of the Doppler search for exoplanets includes only stars of V class luminosity (we recall the confusion with classifying the 51 Peg star as a subgiant).

In atmospheres of chemically peculiar stars of some types, regions of concentration of some elements (and their ions) are observed in which the corresponding spectral lines are predominantly formed. Therefore, the positions of lines for different elements determined by the visible hemisphere of the stellar atmosphere are different. The accuracy of the 'comprehensive' application of the cross-correlation technique, i.e., for all spectral lines of such stars, is then limited. The axial rotation and nonradial pulsations of a 'spotted' star cause variations in the line shape, and, in the case of insufficient spectral resolution, modulate the positions of line cores [194, 195]. The frequencies observed in the spectra of rapidly oscillating peculiar roAp stars agree well with model spectra [196]. A close neighbor with the orbital radius 0.5 AU and mass $0.5M_{\odot}$ was discovered for one of the rapidly oscillating peculiar stars [197], which will affect the strategy of the spectroscopic monitoring of roAp stars. The gravitational redshift in the atmospheres of stars with different luminosities changes by three orders of magnitude: from 30 km s^{-1} for white dwarfs to 30 m s^{-1} for supergiants [198]. Because of the inaccuracy in determining the gravitational acceleration by the method of atmospheric models, the star radius and mass cannot be determined with an accuracy of better than 5%, and the gravitational shift for a single star cannot be calculated with an accuracy of better than 50 m s^{-1}. A close satellite can affect the shape of spectral lines of the central star due to the reflection effect [199]. The type of perturbations of line profiles can be used to determine the orbit inclination angle and then the satellite mass. The method also allows determining the combination of the satellite radius and albedo. The required accuracy of recording line profiles is at present the best achievable.

The study of the spectrum of stellar pulsations is essentially the only method for obtaining empirical information on the mass distribution along the star radius (which can also be obtained from the rotation of the line of apsides in binary systems). Pulsation spectra in asteroseismic studies are obtained during long continuous observations with the help of a longitudinally distributed network of telescopes. The WET (Whole Earth Telescope) program [200, 201], in which coordinated photometric observations of the same object were performed on different continents, has been successful.

The problem of *spectroscopic* asteroseismic observations is also complicated by the fact that to provide continuous series, large-diameter ($D \sim 2-4$ m) telescopes equipped with spectroscopic instruments of the same type are required. These telescopes should operate by consistent observation programs. One of the first attempts at asteroseismic observations was the MuSiCoS program (Multi-Site Continuous Spectroscopy) [202], developed consistently in Europe, Hawaii, and China using 2-meter telescopes equipped with spectrographs of the same type. The restriction on the diameter of a telescope used in experiments is determined by the signal accumulation time for each of the spectra. During long exposures, it is impossible to separate high-frequency pulsation harmonics. It is known that different oscillation modes can be excited and can decay, and the amplitude of the radial velocity can vary from night to night [85].

9. Properties of parent stars

If spectroscopists cannot provide the required Doppler accuracy, they can study the problem of formation of exoplanets by analyzing the chemical composition of the atmospheres of stars for which exoplanets have already been found. Planet formation models can be divided into two types: the core accretion model [203–205] and the disk instability model [206, 207]. The scenario of core accretion for solid, metal-rich particles is confirmed by the dominance of planets around stars with enhanced metallicity [208–218]. However, giant planets were also discovered for stars with lower metallicity [219, 220]. The correlation between metallicity and the proportion of stars with planets is well established only for giant planets, whereas for stars with planets of Neptune's mass and super-earths, such a correlation has not been observed so far. The chemical composition of stellar atmospheres was studied in [221] using the spectra of 1111

stars of the FGK spectral classes obtained with the HARPS spectrograph [34]. Stars for which planets had not been discovered by then were compared with those for which both neptunes and super-earths (26 stars) or massive planets (109 stars) had been discovered. It was found that in a certain metallicity interval ($[\mathrm{Fe/H}] \leqslant -0.2-0.1$, depending on the chemical element), the relative abundance $[X/\mathrm{Fe}]$ of elements, where $X = \mathrm{Mg}$, Al, Si, Sc, Ti, was systematically higher than that for stars without planets. This is expressed most distinctly for Mg.

The authors of [222] studied the abundance of Li in stars that are 'twins' of the Sun in the spectral class and the luminosity class. It was shown that the average content of Li in 22 stars was lower than in 60 stars used for comparison. Because the parameters of all the stars are located in narrow intervals ($\Delta T_\mathrm{e} = 80$ K, $\Delta \log g = 0.2$, where T_e is the effective temperature of the atmosphere, g is the surface gravity, and $\Delta[\mathrm{Fe/H}] = 0.2$), it was concluded that the presence of planets induces additional mixing in star envelopes. If the mixing occurs in layers with conditions sufficient for lithium to burn out, the content of lithium in the atmosphere decreases. The degree of lithium depletion is higher for stars with planets exceeding Jupiter in mass.

In [223], a correlation between the metallicity and the presence of a planet was considered for giant stars. The parameters of the atmospheres of evolved stars with planets (71 stars) were re-evaluated based on two lists of lines. For red giants ($\log g < 3.0$) with planets, no signs of metal enrichment were found compared with red giants without planets. Five known rocky planets (Kepler-10b, Kepler-36b, Kepler-78b, Kepler-93b, and COROT-7b) with masses measured with a high accuracy (which is still some 20%) fall to one line on the $M-R$ (mass-radius) diagram [224] corresponding to the model of a planet consisting of 17% iron and 83% silicates. This relation agrees with an accuracy of 20% with estimates of the Fe content obtained in [225] for Earth (36%), Venus (30–36%), and Mars (23–25%).

In the condensation planet formation model, the relative abundance of elements within small distances from the star (~ 1 AU) does not change. If it was possible to compare the abundance of iron and other elements in the star atmosphere and in the planet model, it would be possible to obtain a key for determining the relation between Fe and other elements for earth-like planets. In [226], the abundance of Fe, Si, Mg, O, and C was determined in the atmospheres of three stars: CoRoT-7, Kepler-10, and Kepler-93. If the relation between the planet core mass (obtained from the mass–radius relation) and the chemical composition of the star is confirmed for a more representative sample, we will gain the potential to estimate the internal structure of earth-like planets.

Thus, the determination of the chemical composition of stars is important not only for studying the structure of planetary systems but also for determining the internal structure and chemical composition of planets. Accurate spectroscopic parameters for stars with planets from the WASP (Wide Angle Search for Planets) review are obtained in [227]. The limit accuracy of measuring atmospheric parameters ($\Delta T_\mathrm{e} = 83$ K, $\Delta \log g = 0.11$, microturbulent velocity $\Delta V_\mathrm{t} = 0.11$ km s^{-1}, and $\Delta[\mathrm{Fe/H}] = 0.10$) independently of the signal-to-noise ratio (S/N) in the spectrum has been found. It was concluded that the metallicity [Fe/H] obtained from spectra with a lower S/N is overstated, which is, in our opinion, rather trivial (see, e.g., [228, 229]).

10. Spectroscopy of transit phenomena. Atmospheres of exoplanets

The transit phenomenon was first defined only as a photometric effect of eclipsing the star disk by the planet disk, when the relative depth of the light curve minimum is independent of the efficient wavelength of a filter. When an exoplanet has an extended atmosphere, observations in different photometric bands can lead to the discovery of chromatic variations of the light curve shape (i.e., the presence of different eclipsing depths and durations in different rays). In some cases, based on broadband photometry in the visible and IR ranges, the average density of an exoplanet (see, e.g., [230]) and the average molecular weight of its atmosphere (see, e.g., [213]) were estimated. Such estimates require very carefully simulating the darkening of the star disk toward its edge, especially in photometric bands where molecular absorption is observed. The observations of four transits of the HD 209458b planet performed with the STIS (Space Telescope Imaging Spectrograph) [232] of the HST telescope gave four eclipse curves in 10 spectrophotometric bands in the range 2,900–10,300 Å [233]. In spectroscopic studies of transit phenomena, the main observational index is the 'spectral ratio' $\mathcal{R}(\lambda)$ obtained for spectra recorded during the transit and in its absence.

The main factor determining $\mathcal{R}(\lambda)$ is the wavelength dependence of the height at which the atmosphere of a giant planet becomes opaque for tangential beams. Strictly speaking, the planet radius is different at each wavelength, and therefore the transit depths are different. Similarly to the atmospheres of Solar system planets, the atmospheres of extrasolar giant planets (EGPs) can consist of molecular mixtures (H_2, CO, H_2O, CH_4), and near-IR bands are the most convenient for diagnostics. However, spectrographs developed for high-precision Doppler measurements of stars by atomic lines in the visible range are not optimal for near-IR studies (in some such spectrographs, this wavelength range remains 'off scene'). Traces of the atmosphere can also be searched for by the cores of resonance lines of alkali metals. However, it is difficult to determine the parameters of the molecular atmosphere from small additions of these elements. The author of [234] used the example of the HD 209458b object to consider the model of the transit phenomenon for the EGP atmosphere consisting of H, C, N, and O, assuming hydrostatic and chemical equilibrium and absorption in the CO, H_2O, and CH_4 bands. Requirements for the spectral data were rather high: $\mathrm{S/N} > 10^3$. The spectral resolution was $10^3 < R < 10^6$.

We note that the duration of a transit phenomenon restricts the attainability of these parameters in middle-diameter telescopes. The core accretion theory predicts the possibility of the formation of a large number of earth-like planets for low-mass stars with a small size of accretion protoplanetary disks, which have not been observed so far for two reasons. First, the observation of such low-mass stars with low luminosity (brown or even cooler dwarfs whose interior temperature is insufficient for hydrogen burning reactions) is a certain problem. Second, the photometric search for transit phenomena in such stars should be performed in the near-IR range, where the accuracy of measurements depends on variations in the content of water vapor (precipitated water) in Earth's atmosphere. By simulating variations in precipitated water in the problem of long-term photometry and spectroscopy of M stars, the authors

of [235] showed that spatial and temporal inhomogeneities of precipitated water can provide a change in the brightness by 0.003–0.004 of the stellar magnitude in the photometric z band of the SDSS (Sloan Digital Sky Survey), comparable to a signal from the transit of a super-earth over the disk of a star of the middle subclass M. The characteristic time of transparency variation in Earth's atmosphere is comparable to the transit time. It was found in [26] by the method of transit photometry that a star with an effective temperature below 2700 K located at a distance of 12 pc from Earth has three Earth-like short-period planets.

The definition of transit can be expanded to include reflection effects. The study of the HD 20782 system with the maximal eccentricity of 0.97 [166] showed that phase variations of brightness are caused by reflection that manifests itself near the periastron. In addition, the expanded definition of transit phenomena also includes *variations in the spectrum* of the parent star caused by the eclipse of the star disk and reflection and transmission of the planet atmosphere.

Here, in addition to [234], we present several examples. We recall the *Rossiter–McLaughlin* (RM) effect. Studies of the radial velocity curves of binary systems revealed deviations caused by the axial rotation of the eclipsed component. During successive eclipses of the disk parts moving towards and away from the observer, the radial velocity curve exhibited deviations in the opposite directions. The deviation amplitude is 26 km s^{-1} for the β Lyrae system [237] and 35 km s^{-1} for the β Persei system [238]. Measurements of the rotation effect in binary systems can be used to determine the size of the eclipsed system, whereas analysis of the photometric light gives only relative dimensions. When a planet passes between the observer and the star, part of the star's surface is eclipsed. This distorts the shape of stellar spectrum lines and causes small variations (a few dozen meters per second) in the radial velocity. When the star disk is eclipsed by the exoplanet, it is possible to determine the angle between the normal to the planet orbit and the rotation axis of the star. Systems in which this angle is small are mainly encountered for cool stars with $T_e < 6250$ K [239, 240].

It was shown that the temperature threshold of the transition to 'adjusted' orbits (coplanar to the star equator) is related to a change in the internal structure of stars, when the external convective envelope becomes responsible for tidal interactions [241]. The authors of [242] determined the angles of inclination of the axial rotation of the star to the orbital plane and made assumptions about the dynamic history of two systems (WASP-13 and WASP-32). If the radial velocities in the transit phenomenon are determined in a broad wavelength range, it is possible to measure the slope of the *transmission spectrum* formed by the planetary atmosphere. In [243], the chromatic component of the RM effect (changes in the shape of the radial-velocity-deviation curve depending on 500 Å subranges) was measured in three series of observations of transits of the HD 189733b planet. Under the assumption that the only cause of the wavelength dependence of the planet–star radial ratio is Rayleigh scattering, the height scale and temperature of the atmosphere were estimated to be 2300 ± 900 K.

In [244], a model of the RM effect was used without assumptions about the shape of lines based on stable point diagrams of the HARPS spectrograph [34]. The model of rigid axial rotation of the star was discarded in application to the HD 189733 object, and a conclusion was reached about the absence of variations of line profiles from the disk center to the limb. For six hot jupiters from the WASP review, the use of models based on measurements of radial velocities in the RM effect (the Boué [245] and Hirano [246] models) and Doppler tomography allowed determining the parameters of orbital rotation, and a planet on a retrograde orbit was observed [247]. It was shown in [248] that light reflected from a planet on a low orbit makes a noticeable contribution to the shape of the stellar spectrum, this contribution moving over the line profile, depending on the projection of the planet rotation velocity.

A giant planet ($R = 1.2R_J$) rotating with a period of 3.5 days around the τ Boo star at a distance of 0.046 AU can reflect 0.01% of the light emitted by the star. The amplitude of variations in the radial velocity of the planet is 152 km s^{-1}, which results in changes in the bisector shape for the stellar spectrum line. Observations of τ Boo (m = 4.5) on the HIRES spectrograph of the 10-meter Keck telescope were performed by adopting special measures for the distribution of the spectrum image on a detector across the main dispersion [176]. The model was also constructed for the case where a planet locked by tidal interaction reflects a copy of the star spectrum not broadened by the axial rotation of the planet.

In [249], the *reflection spectra* of the 51 Peg system were found. The planet mass was estimated as $0.46M_J$ and the orbit plane inclination was approximately determined. For the high albedo value of 0.5, the planet radius was $1.9R_J$. The signal amplitude separated from the star spectrum was 6×10^{-5}. Observations of such spectroscopic effects are restricted by the duration of transit phenomena and are the strongest argument for increasing the efficiency of high-resolution spectroscopy on the existing and projected large telescopes (the ESPRESSO (Echelle SPectgrograph for Rocky Exoplanet and Stable Spectroscopic Observations) project with VLTs and HiReS and METIS (Mid-Infrared E-ELT-Imager and Spectrograph) projects with the E-ELT (European Extremely Large Telescope)).

We note that for high-resolution spectroscopy with large telescopes, bright nights are traditionally allotted at Moon phases between the first and the last quarter. On such nights, the solar light reflected from the Moon and scattered by a thin mist can make a contribution to the star spectrum at a level of 10^{-3}.

The influence of an inhomogeneous cloud cover of the exoplanet on the shape of the *transmission spectrum* in the range 1.1–1.7 μm was considered in [250]. The possibilities of the spectroscopy of transit phenomena in molecular bands with a moderate spectral resolution are strongly limited by the cloud cover. The Na atoms, which are also present above the clouds, are a good object for studying the upper layers of the atmosphere. The high-resolution ($R = 115{,}000$) transmission spectra of the atmosphere of one of the best studied exoplanets, HD 189733b, were obtained in [251]. Traces of the atmospheric spectra of the exoplanet (excessive absorption at 0.32% within bins 0.75 Å in width) were distinguished in the lines of the resonance NaI doublet. For two heights, the temperature was estimated as ∼ 3000 K, which increased with decreasing density.

The spectroscopy of giant planets in low orbits allows combining Doppler tomography and the photometry of transits. The authors of [252] studied a hot jupiter rotating with a two-day period around the FIV star having a high axial rotation velocity ($V \sin i = 52$ km s^{-1}). Here, spectroscopy is used not for Doppler measurements but for recording variations in the spectral line shape caused by the planet transit over the star disk. The WASP–167/KELT-13 system

(described simultaneously in two reviews) is one of the few in which the axial rotation period of the star is shorter than the planet rotation period. Nonradial δ Scuti-type stellar pulsations were found.

Not all spectroscopists studying the physics of stellar atmospheres were 'converted' into researchers of exoplanets, retaining their interest in the field of stellar evolution. To refine calculations of the chemical composition and analysis of vibrational spectra, three-dimensional hydrodynamic models of stellar atmospheres have been developed. Previously, the results of simulations could be verified only by comparing theoretical and observed bisectors of spectral lines recorded from the visible hemisphere of a star [190], but today it is possible to record the spectra of the hemisphere when parts of it are successively eclipsed by the planet disk. Papers [253, 254] open up the field of reconstructing the structure of the eclipsed surface. For normal stars, the ratio of line profiles at different phases of the transit differs by 0.5%, which requires the unrealistic S/N > 5000. In the spectra of cool stars, many lines with similar formation conditions can be found, which allows reducing the accuracy requirements for an individual profile.

The authors of [255] reconstructed the spectra of parts of the HD 209458 surface eclipsed by the HD 209458b satellite — the first exoplanet (Osiris) discovered by the photometric transit method [163]. From several hundred archival transit spectra obtained with the largest telescopes, observations performed on 14.08.2006 with the UVES (Ultraviolet and Visual Echelle Spectrograph) of the VLT ($R = 80000$, $S/N \sim 500$) are selected for studying Osiris's atmosphere. The profiles of FeI lines with different intensities were compared with model profiles. The COSSBOLD calculation code [256] covers the spatial scale from subgranular to the star diameter, and the temporal scale from the period of photosphere waves to the axial rotation period of the star or the duration of the dynamo cycle. Deviations from the local thermodynamic equilibrium are also taken into account. The search for effects related to the exocomet hypothesis can also be assigned, based on the observation technique, to the spectroscopy of transit phenomena. Rapidly rotating A stars episodically exhibit envelope TiII lines in the range of ground-based UV observations [257]. This effect is observed for a quarter of the stars with $V \sin i > 175$ km s^{-1}. During the 22-year monitoring, these lines disappeared and reappeared, the characteristic time of variations exceeding one year [258]. Because of the high excitation potential of ion lines, the phenomenon is ascribed to the presence of hot internal disks in the vicinity of young (less than 50 million years) A stars. One third of the main-sequence A stars emit excessive IR radiation, interpreted as a manifestation of cold external dust disks. The dust can be produced due to selective condensation of atoms and ions escaping from the star [259] and the sublimation of icy bodies [260]. In the vicinity of hot stars, the second scenario is more suitable. The search for signs of the instability of the gas component performed in the K CaII line revealed variations from night to night [261]. This instability is ascribed to individual exocomet evaporation events [262].

11. Promising methods of spectroscopic observations

In this review, we restrict ourselves to assessing the prospects of technological tools and methods, leaving the formulation of problems and interpretation of observations to other colleagues. During the 20th century, astronomical spectroscopy was developed in the direction of increasing the collimated beam diameter d in spectrographs [263], which provided a proportional increase in the spectral resolution R and (or) the spectrograph throughput L. The examples of spectroscopic exoplanet studies presented in Sections 5–10 show that the tendency of increasing d ceased at the maximal value $d \sim 200$ mm. Observations were already separated into two fields: Doppler studies and detailed investigations of line profiles. In the first case, it is sufficient to provide a spectral resolution in the range $40{,}000 < R < 100{,}000$ (on EDLODIE and HARPS spectrographs, respectively), but in the second case, it is necessary to have $R \geqslant 3 \times 10^5$ [155].

In 2018, two spectrographs began to operate: the PEPSI (Potsdam Echelle Polarimetric and Spectroscopic Instrument LBT (Large Binocular Telescope) [264] with $R = 2.7 \times 10^5$ and the ESPRESSO VLT [265] with $R = 225{,}000$. The advantage in R in diffraction instruments leads to the proportional loss in the flux L. We suppose that it is necessary to pass from $R = 10^5$ to $R = 2 \times 10^5$ in a classic diffraction instrument. If this is done using a camera with a doubled focal distance, the illumination of each element of the photodetector would decrease by four times (assuming that the loss level at the spectrograph entrance remains unchanged). The problem of ultrahigh spectral resolution observations of stars is also solved at the expense of certain losses in L, but increasing R is always more advantageous: the final result in astronomical spectroscopy is not the detected flux L but parameters of spectral lines (equivalent linewidths, Doppler shifts, and line profiles).

As an example, we consider the problem of determining the barium isotope ratio from the total profile of the $\lambda = 4554.0$ Å BaII line [266]. Calculations show that the accuracy of measuring the isotope ratio equal to 5% can be obtained for $S/N = 1800$ when $R = 5 \times 10^4$, for $S/N = 460$ when $R = 10^5$, and for $S/N = 250$ when $R = 2 \times 10^5$ [267]. Thus, on passing from $R = 10^5$ to $R = 2 \times 10^5$, the exposure time does not increase, and moreover this time can be *reduced* by a factor of 3.4! The reason for this advantage is the 'oversampling of the line profile' when the line profile elements are distributed among the doubled number of detector elements. The decrease in the exposure time with increasing R is also manifested during Doppler shift measurements. It was shown for the same spectrograph with the same detector for three values of R that the radial velocity measurement error is $\sigma_V \sim R^{-1}$ [116], which agrees well with the results of model calculations. By oversampling the line, the spectral resolution can be increased until detector noise becomes the decisive factor [268].

Therefore, the main promising area in the spectroscopy of stars with exoplanets is the *further increase in the spectral resolution* ($R > 2 \times 10^5$). The spectral resolution of a diffraction spectrograph can be increased by placing a tunable Fabry–Pérot interferometer into a collimated beam [269–271]. Although gaining about an order of magnitude in the spectral resolution, we lose the same due to the nonsimultaneous recording of all spectral elements and transmission losses in the FPI instrumental function peaks. Another factor is the *wavelength range expansion* in the synchronous recording regime. For example, to include the effect of active regions on Doppler measurements performed in the visible spectral range, parallel measurements are required in the ground-based UV range in the K CaII line region.

Statistics of the discovery of super-earths can be improved by increasing the Doppler measurement accuracy. However, another method also exists: low-mass planets can be found more easily in systems of M dwarfs (with a mass of $(0.6-0.075)\,M_\odot$). The middle of the habitable zone of a star with a mass of $0.15M_\odot$ is located at a distance of 0.055 AU [272]. A planet with Earth's mass in such an orbit would be changing the radial velocity of M dwarfs with a period of 12 days and the half-amplitude not greater than 1 m s^{-1}. However, the brightness of M dwarfs in the visible range is a few stellar magnitudes weaker than in the near-IR range (the M6V star at a distance of 10 pc has $m_V \sim 15.5$, whereas $m_K \sim 8.5$ in the 2 μm transparency window).

To perform a spectroscopic survey of the nearest M dwarfs of the southern sky (the Doppler accuracy is 1 m s^{-1} for the 0.5 h signal accumulation time from a star with a stellar magnitude not less than $m_V = 16.5$), the MAROON-X (Magellan Advanced Radial velocity Observer Of Neighboring eXoplanets) spectrograph was constructed for the 6.5-meter Magellan telescope [273] operating in the 5000–9000 Å range with $R = 8 \times 10^4$. Advancement to the near-IR range is also necessary to take spots into account (spots appear to have less contrast at longer wavelengths, and therefore the influence of spots on the results of Doppler measurements is reduced). The near-IR range contains molecular bands expected in the atmospheres of exoplanets. Transit effects in these bands should be more pronounced than in the cores of resonance lines in the optical range. In the near-IR range, several adaptive systems operate stably, which increases the sensitivity of spectrographs used in existing telescopes.

The short-term prospects for high-resolution spectroscopy are related to a major upgrade of the CRIRES (Cryogenic InfraRed Echelle Spectrograph) of the VLT [274, 275]. Problems with internal calibration have been solved by using an absorption cell filled with ammonia vapor [276]. The main problem with near-IR studies is accounting for the telluric spectrum, more exactly, its variable component, the water vapor spectrum. Earth's atmosphere is strongly unsaturated and a sufficient volume remains for local changes in the water vapor content. Modern methods for water vapor monitoring and characteristics of the spatial and temporal variations in the humidity field are described in [227, 278]. It was shown in [279] that the telluric spectrum is simulated with an accuracy of 2%, and in a number of cases the simulation can replace observations of standard stars.

One of the results of the independent development of photometric and spectroscopic methods is the considerable differences among the stars studied in each sample of selected stellar magnitudes. For example, the brightness threshold of a sample in the photometric review of the Kepler mission is $m_V \sim 10$ [280], which is near the lower operation threshold of most facilities used for high-precision Doppler measurements. Therefore, to increase the potential of Doppler spectroscopy, it is necessary to either create specialized instruments with a larger diameter or increase the efficiency of the existing telescopes. The main strategy of increasing the efficiency of ground-based telescopes is the use of image correction. Therefore, we believe that the third factor determining the prospects of exoplanet spectroscopy is *adaptive correction*, providing a drastic decrease in losses at the entrance to a high-resolution spectrograph. For the 3.5-meter SOR (Starfire Optical Range) telescope, an echelle spectrograph with adaptive correction (Airborne Cavity Enhanced Spectrometer (ACES)) with $R = 2 \times 10^5$ was developed [281], which was tested in 1.5- and 2.5-meter telescopes at the Mount Wilson Observatory. The adaptive correction of the star image at the spectrograph entrance leads to revolutionary changes in the classical spectroscopy technique. First, decreasing the entrance-slit width several-fold allows the collimated beam diameter d not to be increased, and the spectrograph (whose cost is proportional to d^3) becomes cheaper. Second, due to a decrease in the working height of the slit, the number of spectral orders that can be packed into the detector is several times greater than in the case without correction. The increase in the number of simultaneously recorded orders reduces (or completely eliminates) the necessity of changing the recorded range and reduces the role of instrumental effects appearing during the instrument readjustment. Finally, due to the narrower slit, the contribution of the inherent night sky radiation decreases (see details in [282]), which is fundamentally important for separating the exoplanetary component from the spectrum of a relatively weak star.

The advantage of ACES is its coupling to a telescope via a single-mode optical fiber (with a 10 μm core), which drastically increases the Doppler accuracy. In multimode fibers, the center of gravity of the illuminated output end of the fiber is displaced due to the interaction of modes, which restricts the Doppler accuracy and requires the use of optical scramblers of different types [283, 284]. The use of single-mode fibers opens up a fundamentally new possibility of constructing high-resolution spectrographs for next-generation giant optical telescopes. The invention of a 'photon lantern', a fiber-optic device with a multimode input and several single-mode outputs, has made it possible to develop single-mode, high-resolution spectrographs with a collimated beam diameter ($d = 22$ mm [286]) a few times or an order of magnitude smaller than in multimode fiber-optic high-resolution spectrographs considered in [287].

We note that the absorption cell method does not yield to the methods based on various fiber-optic systems. An example of a modern facility operating in the automatic Doppler measurement regime is APF (Automatic Planet Finder), consisting of a 2.4-meter telescope and an autocollimation Levy spectrograph ($R \leqslant 1.5 \times 10^5$) [288]. Unlike the best fiber-optically coupled systems (HARPS [34], SOPHIE (from French: Spectrographe pour l'Observation des PHénomènes des Intérieurs et des Exoplanetes) [134], the Levy spectrograph operates with an iodine cell and also provides a Doppler accuracy better than 1 m s^{-1}, but for a shorter signal accumulation time. The use of the absorption cell reduces requirements for the stabilization of conditions in the volume occupied by the optomechanical scheme of the spectrograph.

The statistics of spectroscopic discoveries of exoplanets can be improved by passing to multiobject methods (performing the spectroscopy of several stars in the field of view of the telescope simultaneously). Light from each star can be delivered through an optical fiber at the entrance to a spectrograph with a high slit, recording the same spectral interval for each object [289]. In this case, the main instrumental errors of an echelle spectrograph are preserved.

A more efficient solution is the use of a white light Externally Dispersed Interferometer (EDI). The idea of using an interferometer in precision Doppler measurements proposed and realized in observations of the solar photosphere [290, 291] back in the epoch of one-channel detectors

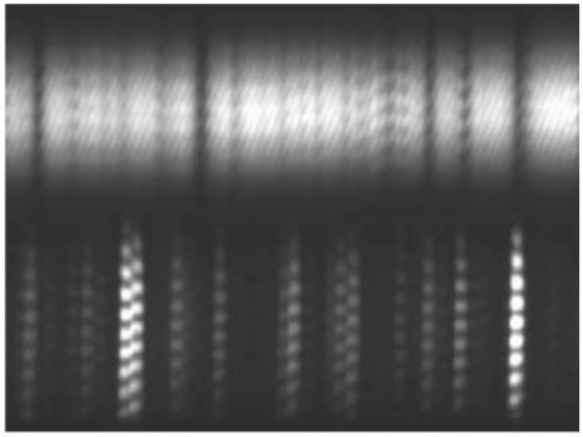

Figure 6. Top: parts of interferograms of the absorption spectrum of a star. Bottom: the emission reference spectrum recorded with an external postdispersion interferometer (EDI) (first experiments; see [293]).

[292] was applied in stellar studies already in the epoch of two-dimensional detectors [293–295]. In the current modification of the method, a white light phase-shifting interferometer is placed not at the exit of a solar diffraction spectrograph but in front of a middle-resolution stellar spectrograph recording one diffraction order. The monochromatic image of a star is elongated over the slit height, and the tilt of one of the interferometer mirrors provides a sinusoidal intensity variation along each line across the dispersion (Fig. 6). The measurement of the shifts of sinusoid parameters along the ordinate (Fig. 6) gives the radial velocity of the star with an accuracy of ~ 1 m s^{-1}. The first exoplanet discovered by the EDI method in the HD 102195 star system ($m_V = 8.05$) was observed with a 0.9-meter telescope [296]. The advantages of the EDI method are the high throughput (in [296], the optical system transmission was 49%), the necessity of stabilization of conditions (temperature and pressure) only within a small interferometer volume, and the possibility of simultaneous Doppler monitoring of several stars in the field of view [297, 298]. For giant planets in low orbits, polarization measurements of radiation reflected by the cloud layer of an exoplanet are possible. Thus, the promising concept of spectropolarimetry [299] using volume-phasing holographic gratings can provide almost 100%-efficient ultrahigh-resolution spectroscopy. This concept allows multiplexing for the simultaneous recording of selected spectral intervals.

Today, the new tasks of spectroscopic exoplanet studies are one of the arguments in favor of the construction of large ground-based telescopes. However, to collect a greater amount of light or to shorten the exposure is not enough: it is also necessary to provide invariable characteristics of a spectrograph for a long time. This problem is also a key one in the development of high-resolution spectrographs used in orbital observatories. The possibilities of orbital spectroscopy are illustrated by the example of the first planet HD 209458b whose atmosphere was discovered spectroscopically during transit.

The STIS HST study with the spectral resolution $R = 5540$ revealed an increase in absorption in the resonance NaI line by 2.3×10^{-4} with respect to the transit decrease in neighboring bands [300]. Later, transit phenomena were observed in the HI, CII, and OI lines [301], demonstrating the intense loss of matter by the planetary atmosphere. The COS (Cosmic Origins Spectrograph) HST study ($R = 17{,}000$) demonstrated a decrease in the radiation flux in the 1334.5323 Å CII, 1335.6854 Å CII, and 1206.500 Å SiIII lines during transit by 8% on average [302]. The CII and SiIII lines are formed at distances up to 2.4 planet radii. The rate of the exosphere matter loss is estimated and a conclusion is made that the content of carbon differs from its content in the atmospheres of giant planets in the Solar system and is close to the solar value. The atmosphere of a planet in the system of the active K spectral type star HD 189733, which is the brightest of the transits, was studied by optical spectra recorded with the STIS HST with a very high signal-to-noise ratio $\sim 11{,}000$ in bands 500 Å wide [303]. The dependence of the planet radius was obtained in the range 2900 – 5700 Å and the effects of the eclipsed and uneclipsed spots modulated by the axial rotation were studied.

However, the same observations of transit phenomena performed with the NICMOS (Near-Infrared Camera and Multi-Object Spectrometer) in the HST gave results that depended on the particular authors [304–308]. The situation improved after passing to the WFC3 (Wide Field Camera 3) in the HST with a detector having a smaller inhomogeneity from pixel to pixel. The HD 189722b exoplanet was observed with the WFC3 in the spectral range 1.1–1.7 μm [309], but, due to the detector nonlinearity and saturation in the central part of the spectrum, the planet/star radial ratio was determined only at the boundaries of the range. The influence of the haze observed with the ACS (Advanced Camera for Surveys) in the HST in the range 0.55–1.05 μm is unnoticeable at wavelengths near 1.1 and 1.7 μm [310]. The WFC3 observations of the atmospheres of the HD 209458b and XO-1b exoplanets revealed traces of water vapor at a wavelength of 1.38 μm attenuated by continuous absorption in the mist [311]. The STIS ($\lambda = 0.29 - 1.03$ μm, $R = 500$) and WFC3 ($\lambda = 1.08 - 1.687$ μm, $R = 130$) observations confirm the presence of water vapor in the WASP-19b atmosphere [312], while the bands of titanium oxide critical for the structure of atmospheres with dominating external radiation [313] were not found. TiO bands are not observed in the WASP-19b atmosphere either, where traces of aerosols were observed [314]. Water vapor bands were found in the spectra of HAT-P-1b, also obtained with WFC3 [315]. Sodium was found in the HAT-P-1b atmosphere from STIS HST observations [316], the pressure broadening effect being absent.

The spectroscopy of a sample of hot jupiters performed with WFC3 HST was developed during the study of the hot uranus GJ 3470b [317]. The IR spectrum does not contain details, which is consistent with ground-based observations and results obtained with the Spitzer telescope [318]. As a whole, according to spectra in the range 0.3–5.0 μm, models of a cloudless hydrogen atmosphere or a hydrogen atmosphere with a haze consisting of tholins (a mixture of organic components formed under the action of UV radiation or cosmic rays important for prebiotic chemistry) are discarded in favor of the cloud atmosphere model rich in hydrogen.

The HD 97658b exoplanet with the orbital period of 9.5 days located at a distance of 0.08 AU from a bright K star offers a rare opportunity of studying the atmosphere of a super-earth (with the mass equal to 7.5 Earth masses). STIS HST observations in the Lyman-α line did not reveal any signs of atmosphere evaporation [319], but demonstrate the fundamental possibility of studying the atmospheres of super-earths.

Most of the mentioned results are model dependent (involving simulations of the stellar spectrum and the planetary atmosphere spectrum [320] and characteristics of spectral instruments). In [321], a new method was proposed and tested for recording the transmission spectra of planetary atmospheres without assumptions about the characteristics of the stellar atmosphere, which can be used in spectral regions with strong contributions from telluric lines. As a whole, the results of orbital spectroscopic studies of exoplanets are obtained at a maximum stretch of the capabilities of the instruments used (with moderate and middle spectral resolution) and are a serious argument for increasing the penetration capability of next-generation orbital telescopes.

12. Outlook for the Spektr-UF mission

Observations in the UV spectral range (115–300 nm) are extensively developed for studying exoplanets and especially exoplanetary atmospheres. At present, the main tool of these studies is the HST, which was put into operation in 1990 and still produces a large amount of observational data, not only in the UV range but also in all spectral ranges studied in astronomy. The outlook for UV astronomy for 2024–2034 between the end of the HST operation in orbit and putting large orbital next-generation observatories into operation is associated with the World Space Observatory–Ultraviolet (WSO–UV) mission (the Russian name of the project is ''Spektr-UF'') [322–324]. The project uses a 1.7-meter Ritchey–Chretien telescope, spectrographs, and a field camera unit. The spectrograph unit has three channels (spectrographs): a high-resolution ($R \approx 5 \times 10^4$) near-UV (176–310 nm) spectrograph, a high-resolution ($R \approx 5 \times 10^4$) far-UV (115–178 nm) spectrograph, and a low-resolution ($R \approx 10^3$) high-slit spectrograph [325–326]. The field camera unit is used for direct imaging in the near and far UV regions [327]. Unlike the observation time in the HST, all the observation time in the WSO–UV is devoted to UV astronomy [328–330]. In addition, this project will work in a geostationary orbit, in fact, above Earth's radiation belts and the geosphere, which itself is a UV-radiation source and considerably complicates such studies. In the period mentioned above, the WSO–UV will in fact be the only 2-meter orbital telescope operating in the UV region.

A major part of the WSO–UV program concerns exoplanet investigations [331, 332]. They can be conventionally grouped into four areas: (a) discovery of planets; (b) studies of planet formation in protoplanetary disks; (c) determination of physical characteristics of planets; and (d) determination of the chemical composition of planetary atmospheres, including biomarkers. The equipment of the Spektr-UF mission is ideally suitable for solving the last three of the listed problems. In addition, exoplanets themselves are a good tool for studying the properties of parent stars, and breakthrough results are also expected in this area of WSO–UV studies. We discuss the potential of the Spektr-UF project to solve these problems in more detail.

Study of planet formation in protoplanetary disks. Key objects for this problem are stars of the T Taurus type. Observations in the far-UV spectral range (115–200 nm) can be used to determine physical and chemical conditions in the internal protoplanetary disk, where a planet is formed and intense H_2 emission and CO lines excited by Ly_α photons are observed. To determine the physical and chemical characteristics of the gas, high-resolution spectra are required. Spectrographs of the WSO–UV mission offer these exact prospects. Compared to COS HST observations, it is necessary to take into account that CCD photodetectors used in the Spektr-UF project have much higher noise than multichannel plate detectors used in the COS. But, at the same time, the spectral resolution of two WSO–UV spectrographs is almost three times greater than the spectral resolution of the COS, which is a significant advantage for detailed studies of emission line shapes.

Determination of physical characteristics of planets: *mass, radius, magnetic field, temperature, pressure*. The UV spectra can be used to study the upper layers of exoplanet atmospheres (the so-called thermosphere and exosphere). Analyses of light curves obtained at different wavelengths before and after the transit of an exoplanet over the parent star disk give the temperature and pressure distributions in the upper atmosphere of the exoplanet. These distributions were determined by using the 121.6 nm HI Ly_α, 133.5 nm CII, and 120.6 nm SiIII lines [302]. In addition, spectral UV observations can be used to study various physical phenomena in the atmosphere, such as photodissociation, the distribution of magnetic fields, and the evaporation of atmospheres [333, 334]. The search for magnetic fields of parent stars [335] will be continued by ground-based instrumentation (see below). Attempts, so far unsuccessful, to determine the magnetic field of exoplanets by auroral phenomena [336] in planetary atmospheres will be continued with the Spektr-UF instruments in a geostationary orbit, which is more convenient for such studies.

Investigation of planetary atmospheres. The COS HST observations in the CII and SiIII lines for the first time revealed the velocity field in the expanding HD 209458b atmosphere and gave an estimate of the mass loss rate [302]. The interpretation of transit spectra directly depends on the variable activity of parent stars observed in the UV range. The advantages of the WSO–UV orbit allowing the detailed long-term monitoring of an exoplanet before and after transit will be decisive. In particular, it will be possible to continuously observe the UV spectra for planets nearest to the star during the total orbital period. Quasi-continuous broadband observations in the IR and visible spectral regions were performed in [337]. Direct measurements of the atomic oxygen content using the 130.5 nm OI line, which are almost free of the influence of Earth's geocorona, as well as the direct WSO–UV measurement of the ozone (O_3) content by absorption in the near-UV range ($\lambda < 350$ nm) will produce data for studying the possibility of the existence of life on exoplanets.

Investigation of properties of parent stars. The UV spectra of stars contain numerous resonance lines of atoms and molecules. The consideration of these lines and determination of the energy distribution in the UV range are very important for reliable measurements of the parameters of stellar atmospheres, the effective temperature, and surface gravity, which are usually determined by lines in the visible spectral region. Exoplanets, especially the most massive and closest to parent stars, affect the characteristics and evolution of these stars. In particular, the tidal interaction between planets and their parent stars can significantly affect the rotation period of a star and its chromosphere activity, producing modulation in accordance with the orbital period of the planet [338]. WSO–UV spectrographs will give long-term continuous series of observation data for monitoring chromosphere and coronal UV emission lines (in particular, the resonance MgII h and k lines at 280 nm), which are much

more sensitive indicators of activity than the optical lines used (for example, the CaII H and K lines or H_α). In exoplanet studies, especially in atmospheric studies, the Spektr-UF mission will be the much-needed working tool. The program of ground-based spectroscopic support developed for the Spektr-UF project relies on available capabilities [339–341] and plans for updating telescopes with modern instruments.

13. Conclusions

The outlook for spectroscopic exoplanet studies in Russian ground-based observatories depends on a number of factors. First, 6-meter [342], 2.65-meter [343], 2.4-meter [344], and 2-meter [345] telescopes are multiprogrammed, and the use of any (including high-cost) spectroscopic instrument with a certain aim may be limited in time. Second, the number of large telescopes is small, and it is difficult to obtain the required observation time for spectroscopy during strictly defined intervals. Third, there is a deficit of highly qualified spectroscopists who can rapidly obtain a new reliable result in the new research field at the limit of the potential of existing instruments. The study of exoplanets quite rapidly became the domain of large research groups. For example, just judging by the references presented in this review, the average number of coauthors more than doubled from six (38 papers in 2006–2010) to thirteen (68 papers in 2011–2015). As pointed out in [346], the development of stellar spectroscopy as a new direction is hampered in Russia by the absence of a specialized spectroscopic telescope equipped with a high-resolution spectrometer and observing only stars, both during dark and moonlit nights. We note that while the Doppler search for exoplanets can be performed during moonlit nights, in most of the spectroscopic problems involving exoplanet atmospheres, the sky background illuminated by the Moon exceeds the planet signal separated from the stellar spectrum during transit phenomena. Therefore, it is likely that some exoplanet programs would claim the dark time of large telescopes, which is in higher demand than bright nights. Obviously, multiprogrammed domestic telescopes mentioned above can be used only episodically and predominantly not for the search for new exoplanet systems but for studying systems that are already known.

Finally, we mention the developments of the SAO, RAS, which can be used to a different degree to search for and study exoplanets. The Nasmyth Echelle Spectrograph (NES) [347] remains the main spectroscopic instrument of the 6-meter BTA. The main characteristics of this spectrograph are being refined according to the program developed [149]. An echelle spectropolarimeter was developed for observations in the prime BTA focus (Echelle-Spectropolarimeter for Prime Focus (ESPriF)) [348–350]. In particular, it can be used to measure linear and circular polarization, avoiding instrumental effects inherent in the NES and the main stellar spectrograph [351] operating in the BTA scheme with a plane mirror. The volume of the BTA prime focus cabin restricts the possibility of accommodating elements for star image correction, which are successfully used in the Nasmyth focus. The original layout of optical elements of the ESPriF and technological solutions for the schemes of echelle spectrographs of the Spektr-UF project [325] can also be acceptable for 2-meter telescopes with suspended high-resolution spectrographs. Following the currently popular idea of fiber-optic coupling between a telescope and a stationary spectrograph, the Ural Fiber Echelle Spectrograph (UFES) was constructed at the SAO [287] for the 1.2-meter telescope of the Ural Federal University, and the manufacture of an Effective Fiber Echelle Spectrograph (EFES) [42, 43] for a 1-meter telescope of the SAO, RAS is being terminated. It is likely that these instruments can also be used for high-precision Doppler studies.

While the results of theoretical studies of planets and exoplanets obtained by Russian scientists are well known (see, e.g., [127, 352–355]), the domestic experimental contribution to exoplanet investigations is barely noticeable so far. It is necessary to analyze the possibilities that exist and to develop a program to update our telescopes based on new instruments developed using new technologies.

Acknowledgments

The study of V E P was supported by the Government of the Russian Federation (grant no. 14.W03.31.0017); the study of V G K was supported by the program of the Presidium of RAS no. 28 "Cosmos: Studies of Fundamental Processes and Their Interactions." The authors thank the referee for the constructive remarks.

References

1. Strand K Aa *Publ. Astron. Soc. Pac.* **55** 28 (1943)
2. Reuyl D *Astron. J.* **45** 133 (1936)
3. Strand K Aa *Publ. Astron. Soc. Pac.* **55** 26 (1943)
4. Strand K Aa *Publ. Astron. Soc. Pac.* **55** 29 (1943)
5. Reuyl D, Holmberg E *Astrophys. J.* **97** 41 (1943)
6. van de Kamp P *Astron. J.* **51** 7 (1944)
7. Deich A N *Izv. Gos. Astron. Observ. Pulkovo* **18** (146) 1 (1951)
8. Struve O *The Observatory* **72** 199 (1952)
9. Barnard E E *Astron. J.* **29** 181 (1916)
10. van de Kamp P *Astron. J.* **67** 284 (1962)
11. van de Kamp P *Astron. J.* **68** 295 (1963)
12. Benedict G F et al. *Astron. J.* **118** 1086 (1999)
13. Choi J et al. *Astrophys. J.* **764** 131 (2013)
14. Vogt S S *Publ. Astron. Soc. Pac.* **99** 1214 (1987)
15. Vogt S S et al. *Proc. SPIE* **2198** 362 (1994)
16. Campbell B, Walker G A H, Yang S *Astrophys. J.* **331** 902 (1988)
17. Astudillo-Defru N et al. *Astron. Astrophys.* **602** A88 (2017)
18. NASA Exoplanet Archive. A service of NASA Exoplanet Science Institute, https://exoplanetarchive.ipac.caltech.edu/
19. Wilson R E *General Catalogue of Stellar Radial Velocities* (Washington, DC: Carnegie Institution of Washington, 1953)
20. Marcy G W, Butler R P *Annu. Rev. Astron. Astrophys.* **36** 57 (1998)
21. Struve O, Elvey C T *Mon. Not. R. Astron. Soc.* **91** 663 (1931)
22. Adams W S *Astrophys. J.* **93** 11 (1941)
23. Petrie R M, Fletcher J M, in *Determination of Radial Velocities and their Applications, Proc. of IAU Symp. No. 30, Toronto, 20–24 June, 1966* (International Astronomical Union. Symp. No. 30, Eds A H Batten, J F Heard) (London: Academic Press, 1967) p. 43
24. Richardson E H, Brealey G A, Dancey R *Publ. Dominion Astrophys. Obs.* **14** 1 (1971)
25. Griffin R *Mon. Not. R. Astron. Soc.* **162** 243 (1973)
26. Griffin R *Mon. Not. R. Astron. Soc.* **162** 255 (1973)
27. Tull R G *Appl. Opt.* **8** 1635 (1969)
28. Panchuk V E et al. *Solar Syst. Res.* **49** 420 (2015); *Astron. Vestn.* **49** 459 (2015)
29. Filippenko A V *Publ. Astron. Soc. Pac.* **94** 715 (1982)
30. Goncharov A V, Devaney N, Dainty C *Opt. Express* **15** 1534 (2007)
31. Klochkova V G et al. *Astrophys. Bull.* **63** 386 (2008); *Astrofiz. Byull.* **63** 410 (2008)
32. Heacox W D, in *Fiber Optics in Astronomy. Proc. of the Conf., Tucson, AZ, Apr. 11–14, 1988* (ASP Conf. Ser., Vol. 3) (San Francisco, CA: Astronomical Society of the Pacific, 1988) p. 204
33. Bouchy F, Connes P, Bertaux J-L, in *Precise Stellar Radial Velocities. IAU Colloquium 170* (ASP Conf. Ser., Vol. 185, Eds

J B Hearnshaw, C D Scarfe) (San Francisco, CA: Astronomical Society of the Pacific, 1999) p. 22
34. Pepe F et al. *Proc. SPIE* **4008** 582 (2000)
35. Wang S et al. *Proc. SPIE* **4841** 1145 (2003)
36. Campbell B, Walker G A H *Publ. Astron. Soc. Pac.* **91** 540 (1979)
37. Campbell B *Publ. Astron. Soc. Pac.* **95** 577 (1983)
38. Cochran W D, Hatzes A P *Proc. SPIE* **1318** 148 (1990)
39. Marcy G W, Butler R P *Publ. Astron. Soc. Pac.* **104** 270 (1992)
40. Panchuk V E, Yermakov S V, Bondarenko Yu N *Bull. Spec. Astrophys. Obs.* **44** 132 (1998)
41. Panchuk V E, Nasonov D S , Yushkin M V *Astrophys. Bull.* **64** 286 (2009); *Astrofiz. Byull.* **64** 297 (2009)
42. PanchukV E et al. *Astrophys. Bull.* **70** 226 (2015); *Astrofiz. Byull.* **70** 237 (2015)
43. Soghoyan H E et al., in *Stars*: *From Collapse to Collapse, Proc. of a Conf., Nizhny Arkhyz, Russia, 3–7 October 2016* (ASP Conf. Ser., Vol. 510, Eds Yu Yu Balega et al.) (San Francisco, CA: Astronomical Society of the Pacific, 2017) p. 554
44. Hearnshaw J B *Observatory* **97** 5 (1977)
45. Gustafsson B, in *ESO Workshop on High Resolution Spectroscopy with the VLT. Proc., Garching, Germany, February 11–13, 1992* (ESO Conf. Workshop Proc., Vol. 40, Ed. M-H Ulrich) (Garching bei Munchen: European Southern Observatory, 1992) p. 17
46. Dunham T (Jr.) *Vistas Astron.* **2** 1223 (1956)
47. Naidenov I D, Panchuk V E, Yushkin M V *Astrophys. Bull.* **62** 296 (2007); *Astrofiz. Byull.* **62** 313 (2007)
48. Brown T M et al. *Publ. Astron. Soc. Pac.* **106** 1285 (1994)
49. Ge J et al. *Publ. Astron. Soc. Pac.* **114** 879 (2002)
50. Connes P, Martic M, Schmitt J *Astrophys. Space Sci.* **241** 61 (1996)
51. Fellgett P *Opt. Acta* **2** 9 (1955)
52. Griffin R F *Astrophys. J.* **148** 465 (1967)
53. Karsten L, in *Proc. of ESO-CERN Conf. on Auxiliary Instrumentation for Large Telescopes, Geneva, May 2–5, 1972* (Eds S Laustsen, A Reiz) (Geneva: CERN, 1972) p. 185
54. Stilborn J R, Fletcher J M, Hartwick F D A *J. R. Astron. Soc. Canada* **66** 49 (1972)
55. Griffin R F, Gunn J E *Astrophys. J.* **191** 545 (1974)
56. van Gitters G W, Warner B *Mon. Not. R. Astron. Soc.* **168** 469 (1974)
57. Beavers W I, Eitter J J *Publ. Astron. Soc. Pac.* **89** 733 (1977)
58. Slovak M H, van Gitters G W, Barnes T G *Publ. Astron. Soc. Pac.* **91** 840 (1979)
59. Fletcher J M et al. *Publ. Astron. Soc. Pac.* **94** 1017 (1982)
60. Walraven Th, Walraven J, in *Proc. of ESO-CERN Conf. on Auxiliary Instrumentation for Large Telescopes, Geneva, May 2–5, 1972* (Eds S Laustsen, A Reiz) (Geneva: CERN, 1972) p. 175
61. Griffin R F *Observatory* **97** 9 (1977)
62. Baranne A, Mayor M, Poncet J L *Vistas Astron.* **23** 279 (1979)
63. Tokovinin A A *Sov. Astron.* **31** 98 (1987); Tokovinin A A *Astron. Zh.* **64** 196 (1987)
64. Upgren A R, Sperauskas J, Boyle R P *Baltic Astron.* **11** 91 (2002)
65. Latham D W et al. *Nature* **339** 38 (1989)
66. Latham D W, in *Instrumentation for Astronomy with Large Optical Telescopes, Proc. of IAU Colloq. 67, Zelenchukskaya, USSR, September 8–10, 1981* (Astrophysics and Space Science Library, Vol. 92, Ed. C M Humphries) (Dordrecht: Springer, 1982) p. 259
67. Serkowski K *Icarus* **27** 13 (1976)
68. Serkowski K *Postepy Astron.* **24** 3 (1976)
69. Serkowski K, in *High Resolution Spectrometry. Proc. of the 4th Intern. Colloquium on Astrophysics, Trieste, July 3–7, 1978* (Ed. M Hack) (Trieste: Osservatorio, 1978) p. 245
70. Serkowski K et al. *Proc. SPIE* **0172** 130 (1979)
71. Serkowski K et al. *Astrophys. J.* **228** 630 (1979)
72. Connes P *Astrophys. Space Sci.* **110** 211 (1985)
73. Flint G *Sky Telesc.* **67** 402 (1984)
74. Isaak G R *Nature* **189** 373 (1961)
75. Roddier F *Ann. Astrophys.* **28** 463 (1965)
76. Fossat E, Roddier F *Solar Phys.* **18** 204 (1971)
77. Grec G, Fossat E, Vernin J *Astron. Astrophys.* **50** 221 (1976)
78. Brookes J R, Isaak G R, van der Raay H B *Mon. Not. R. Astron. Soc.* **185** 1 (1978)
79. Fossat E et al. *C. R. Acad. Sci. II* **299** 17 (1984)
80. Schmider F X et al., in *Advances in Helio- and Asteroseismology, Proc. of the Symp., 17–11 July 1986, Aarhus, Denmark* (IAU Symp., No. 123, Eds J Christensen-Dalsgaard, S Frandsen) (Dordrecht: D. Reidel Publ. Co., 1988) p. 513
81. Tull R G, Choisser J P, Snow E H *Appl. Opt.* **14** 1182 (1975)
82. Vogt S S,Tull R G, Kelton P *Appl. Opt.* **17** 574 (1978)
83. Beckers J M *Astrophys. J.* **213** 900 (1977)
84. Koch A, Wöhl H *Astron. Astrophys.* **134** 134 (1984)
85. Libbrecht K G *Astrophys. J.* **330** L51 (1988)
86. Cochran W D, Hatzes A P, in *Planets Around Pulsars, Proc. of the Conf., California Inst. of Technology, Pasadena, Apr. 30 – May 1, 1992* (San Francisco, CA: Astronomical Society of the Pacific, 1993) p. 267
87. Libbrecht K G *Space Sci. Rev.* **47** 275 (1988)
88. Libbrecht K G, Peri M L *Publ. Astron. Soc. Pac.* **107** 62 (1995)
89. Smith M A *Astrophys. J.* **253** 727 (1982)
90. Smith M A *Astrophys. J.* **265** 325 (1983)
91. Hatzes A P, Cochran W D *Astrophys. J.* **413** 339 (1993)
92. Butler R P, Bell R A, Hindsley R B *Astrophys. J.* **461** 362 (1996)
93. Butler R P, Bell R A *Astrophys. J.* **480** 767 (1997)
94. Walker G A H et al. *Icarus* **116** 359 (1995)
95. Campbell B, Walker G A H, Yang S *Astrophys. J.* **331** 902 (1988)
96. Cochran W D, Hatzes A P *Bull. Am. Astron. Soc.* **22** 1082 (1990)
97. Baranne A et al. *Astron. Astrophys. Suppl.* **119** 373 (1996)
98. Mayor M, Queloz D *Nature* **378** 355 (1995)
99. Hatzes A P, Cochran W D, Johns-Krull C M *Astrophys. J.* **478** 374 (1997)
100. Hoffleit D *Catalogue of Bright Stars* (New Haven, CT: Yale Univ. Observatory, 1964)
101. McMillan R S et al. *Astrophys. J.* **403** 801 (1993)
102. Noyes R W et al. *Astrophys. J.* **483** L111 (1997)
103. Cochran W D, Hatzes A P *Astrophys. Space Sci.* **241** 43 (1996)
104. Walker G A H et al. *Icarus* **116** 359 (1995)
105. Marcy G W, Butler R P *Annu. Rev. Astron. Astrophys.* **36** 57 (1998)
106. Ksanfomaliti L V *Solar Syst. Res.* **34** 481 (2000); *Astron. Vestn.* **34** 529 (2000)
107. Ksanfomaliti L V, in *Istoriko-Astronomicheskie Issledovaniya* (Historical and Astronomical Researches) Issue 27 (Moscow: Nauka, 2002) p. 54
108. Butler R P, Marcy G W *Astrophys. J.* **464** L153 (1996)
109. Marcy G W, Butler R P *Proc. SPIE* **2704** 46 (1996)
110. Marcy G W, Butler R P *Astrophys. J.* **464** L147 (1996)
111. Cochran W D et al. *Astrophys. J.* **483** 457 (1997)
112. Marcy G W et al. *Astrophys. J.* **481** 926 (1997)
113. Delfosse X et al. *Astron. Astrophys.* **338** L67 (1998)
114. Merline W J, in *Stellar Radial Velocities, Proc. of IAU Colloquium No. 88, Schenectady, N.Y., October 24–27, 1984* (Eds A G D Philip, D W Latham) (Schenectady, NY: L. Davis Press, 1985) p. 87
115. Seifahrt A et al. *Proc. SPIE* **9908** 990818 (2016)
116. Hatzes A P, Cochran W D, in *ESO Workshop on High Resolution Spectroscopy with the VLT. Proc., Garching, Germany, February 11–13, 1992* (ESO Conf., Vol. 40, M-H Ulrich) (Garching bei Munchen: European Southern Observatory, 1992) p. 275
117. Dekker H et al. *Proc. SPIE* **4008** 534 (2000)
118. Noguchi K et al. *Proc. SPIE* **3355** 354 (1998)
119. Vogt S S et al. *Publ. Astron. Soc. Pac.* **126** 359 (2014)
120. Noyes R W et al. *Astrophys. J.* **487** L195 (1997)
121. Lissauer J J *Nature* **398** 659 (1999)
122. Safronov V S *Astron. Zh.* **43** 817 (1966)
123. Safronov V S *Solar Syst. Res.* **18** 208 (1985); *Astron. Vestn.* **18** 322 (1984)
124. Wetherill G W *Astrophys. Space Sci.* **241** 25 (1996)
125. Lissauer J J, Marcy G W, Ida S *Proc. Natl. Acad. Sci. USA* **97** 12405 (2000)
126. Woolfson M M *The Origin and Evolution of the Solar System* (Bristol: Institute of Physics Publ., 2000)
127. Bisikalo D V, Kaygorodov P V, Shematovich V I "Exoplanets: Atmospheres of hot Jupiters", in *Oxford Research Encyclopedias. Planetary Science* (Oxford: Oxford Univ. Press, 2019) https://doi.org/10.1093/acrefore/9780190647926.013.103
128. Pfeiffer M J et al. *Astron. Astrophys. Suppl.* **130** 381 (1998)
129. Tull R G *Proc. SPIE* **3355** 387 (1998)
130. Kaufer A, Pasquini L *Proc. SPIE* **3355** 844 (1998)

131. Queloz D et al. *Astron. Astrophys.* **354** 99 (2000)
132. Manset N, Donati J-F *Proc. SPIE* **4843** 425 (2003)
133. Weber M et al. *Proc. SPIE* **7019** 70190L (2008)
134. Perruchot S et al. *Proc. SPIE* **7014** 70140J (2008)
135. Crane J D et al. *Proc. SPIE* **7735** 773553 (2010)
136. Schwab C et al. *Proc. SPIE* **7735** 77354G (2010)
137. Raskin G et al. *Astron. Astrophys.* **526** A69 (2011)
138. Cosentino R et al. *Proc. SPIE* **8446** 84461V (2012)
139. Dominici T P et al. *Proc. SPIE* **8446** 844636 (2012)
140. Chakraborty A et al. *Publ. Astron. Soc. Pac.* **126** 133 (2014)
141. Butler R P et al. *Publ. Astron. Soc. Pac.* **108** 500 (1996)
142. Chountonov G A *Astrophys. Bull.* **66** 496 (2011); *Astrofiz. Byull.* **66** 533 (2011)
143. Osterman S et al *Proc. SPIE* **6693** 66931G (2007)
144. Steinmetz T et al. *Science* **321** 1335 (2008)
145. Steinmetz T et al. *Appl. Phys. B* **96** 251 (2009)
146. Lo Curto G et al. *Proc. SPIE* **8446** 84461W (2012)
147. Phillips D F et al. *Proc. SPIE* **8446** 84468O (2012)
148. Murphy M T et al. *Mon. Not. R. Astron. Soc.* **422** 761 (2012)
149. Panchuk V E, Klochkova V G, Yushkin M V *Astron. Rep.* **61** 820 (2017); *Astron. Zh.* **94** 808 (2017)
150. Abbas M M et al. *Appl. Opt.* **15** 427 (1976)
151. Dravins D *Annu. Rev. Astron. Astrophys.* **20** 61 (1982)
152. Dravins D, Nordlund Å *Astron. Astrophys.* **228** 184 (1990)
153. Dravins D, Nordlund Å *Astron. Astrophys.* **228** 203 (1990)
154. Dravins D *Astron. Astrophys.* **492** 199 (2008)
155. Dravins D *Astron. Nachr.* **331** 535 (2010)
156. Jacquinot P *Rep. Prog. Phys.* **23** 267 (1960); Translated into Russian: *Usp. Fiz. Nauk* **78** 123 (1962)
157. Kulagin E S *Sov. Astron.* **24** 118 (1980); *Astron. Zh.* **57** 200 (1980)
158. Perryman M *Am. J. Phys.* **82** 552 (2014)
159. Sahlmann J et al. *Astron. Astrophys.* **551** A52 (2013)
160. Perryman M et al. *Astrophys. J.* **797** 14 (2014)
161. Rosenblatt F *Icarus* **14** 71 (1971)
162. Henry G W et al. *Astrophys. J.* **529** L41(2000)
163. Charbonneau D et al. *Astrophys. J.* **529** L45 (2000)
164. Hellier C et al. *Mon. Not. R. Astron. Soc.* **426** 739 (2012)
165. Christiansen J L et al. *Publ. Astron. Soc. Pac.* **124** 1279 (2012)
166. Kane S R et al. *Astrophys. J.* **821** 65 (2016)
167. Baranec C et al. *Astrophys. J. Lett.* **790** L8 (2014)
168. Baranec C et al. *Astron. J.* **152** 18 (2016)
169. Abe F et al. *Science* **305** 1264 (2004)
170. Barry R et al. *Proc. SPIE* **8151** 81510L (2011)
171. Holman M J, Murray N W *Science* **307** 1288 (2005)
172. Hrudková M et al. *Proc. IAU* **4** (S253) 446 (2008)
173. Quirrenbach A *Annu. Rev. Astron. Astrophys.* **39** 353 (2001)
174. Trauger J et al. *Proc. SPIE* **8151** 81510G (2011)
175. Udry S, Santos N C *Annu. Rev. Astron. Astrophys.* **45** 397 (2007)
176. Charbonneau D et al. *Astrophys. J.* **522** L145 (1999)
177. Cameron A C et al. *Nature* **402** 751 (1999)
178. Burrows A, Angel R *Nature* **402** 732 (1999)
179. Parsons S B *Astrophys. J.* **174** 57 (1972)
180. Vaughan A H et al. *Astrophys. J.* **250** 276 (1981)
181. Panchuk V E, Klochkova V G, Yushkin M V *Astrophys. Bull.* **65** 269 (2010); *Astrofiz. Byull.* **65** 283 (2010)
182. Haywood R D et al., in *European Planetary Science Congress 2013, 8–13 September, London, UK*, EPSC2013-215; https://meetings.copernicus.org/epsc2013/
183. Queloz D et al. *Astron. Astrophys.* **379** 279 (2001)
184. Els S G et al., in *Scientific Frontiers in Research on Extrasolar Planets* (ASP Conf. Ser., Vol 294, Eds D Deming, S Seager) (San Francisco, CA: ASP, 2003) p. 55
185. Haywood R D et al. *Mon. Not. R. Astron. Soc.* **443** 2517 (2014)
186. Dravins D, Lindegren L, Nordlund A *Astron. Astrophys.* **96** 345 (1981)
187. Dravins D, Larsson B, Nordlund A *Astron. Astrophys.* **158** 83 (1986)
188. Livingston W C *Nature* **297** 208 (1982)
189. Bruning D H *Bull. Am. Astron. Soc.* **16** 577 (1984)
190. Dravins D *Astron. Astrophys.* **172** 200 (1987)
191. Stathopoulou M, Alissandrakis C E *Astron. Astrophys.* **274** 555 (1993)
192. Nordlund A , Dravins D *Astron. Astrophys.* **228** 155 (1990)
193. Atroshchenko I N, Gadun A S *Astron. Astrophys.* **291** 635 (1994)
194. Sachkov M et al., in *Variable Stars in the Local Group, IAU Colloquium 193, Proc. of the Conf., 6–11 July, 2003, Christchurch, New Zealand* (ASP Conf. Proc., Vol. 310, Eds D W Kurtz, K R Pollard) (San Francisco, CA: Astronomical Society of the Pacific, 2004) p. 208
195. Sachkov M et al. *Mon. Not. R. Astron. Soc.* **389** 903 (2008)
196. Saio H, Ryabchikova T, Sachkov M *Mon. Not. R. Astron. Soc.* **403** 1729 (2010)
197. Hartmann M, Hatzes A P *Astron. Astrophys.* **582** A84 (2015)
198. Lindegren L, Dravins D *Astron. Astrophys.* **401** 1185 (2003)
199. Charbonneau D, Jha S, Noyes R W *Astrophys. J.* **507** L153 (1998)
200. Nather R E et al. *Astrophys. J.* **361** 309 (1990)
201. Provencal J L et al. *Contrib. Astron. Obs. Skalnaté Pleso* **43** 524 (2014)
202. Catala C et al. *Astron. Astrophys.* **275** 245 (1993)
203. Pollack J B et al. *Icarus* **124** 62 (1996)
204. Ida S, Lin D N C *Astrophys. J.* **616** 567 (2004)
205. Mordasini C et al. *Astron. Astrophys.* **541** A97 (2012)
206. Boss A P *Science* **276** 1836 (1997)
207. Boss A P *Astrophys. J.* **567** L149 (2002)
208. Gonzalez G *Astron. Astrophys.* **334** 221 (1998)
209. Gonzalez G et al. *Astron. J.* **121** 432 (2001)
210. Santos N C, Israelian G, Mayor M *Astron. Astrophys.* **373** 1019 (2001)
211. Santos N C et al. *Astron. Astrophys.* **398** 363 (2003)
212. Santos N C, Israelian G, Mayor M *Astron. Astrophys.* **415** 1153 (2004)
213. Fischer D A, Valenti J *Astrophys. J.* **622** 1102 (2005)
214. Sousa S G et al. *Astron. Astrophys.* **487** 373 (2008)
215. Neves V et al. *Astron. Astrophys.* **497** 563 (2009)
216. Johnson J A et al. *Publ. Astron. Soc. Pac.* **122** 905 (2010)
217. Sousa S G et al. *Astron. Astrophys.* **533** A141 (2011)
218. Adibekyan V Zh et al. *Astron. Astrophys.* **535** L11 (2011)
219. Cochran W D et al. *Astrophys. J.* **665** 1407 (2007)
220. Santos N C et al. *Astron. Astrophys.* **512** A47 (2010)
221. Adibekyan V Zh et al. *Astron. Astrophys.* **543** A89 (2012)
222. Delgado Mena E et al. *Astron. Astrophys.* **562** A92 (2014)
223. Mortier A et al. *Astron. Astrophys.* **557** A70 (2013)
224. Dressing C D et al. *Astrophys. J.* **800** 135 (2015)
225. Zeng L, Sasselov D *Publ. Astron. Soc. Pac.* **125** 227 (2013)
226. Santos N C et al. *Astron. Astrophys.* **580** L13 (2015)
227. Doyle A P et al. *Mon. Not. R. Astron. Soc.* **428** 3164 (2013)
228. Klochkova V G, Panchuk V E *Sov. Astron. Lett.* **11** 291 (1985); *Pis'ma Astron. Zh.* **11** 692 (1985)
229. Panchuk V E, Tsymbal V V *Bull. Spec. Astrophys. Obs.* **20** 18 (1985); *Astrofiz. Issled. Spets. Astrofiz. Observ.* **20** 22 (1985)
230. de Mooij E J W et al. *Astron. Astrophys.* **538** A46 (2012)
231. Croll B et al. *Astrophys. J.* **736** 78 (2011)
232. Kimble R A et al. *Astrophys. J.* **492** L83 (1998)
233. Knutson H A et al. *Astrophys. J.* **655** 564 (2007)
234. Brown T M *Astrophys. J.* **553** 1006 (2001)
235. Blake C H, Shaw M M *Publ. Astron. Soc. Pac.* **123** 1302 (2011)
236. Gillon M et al. *Nature* **533** 221 (2016)
237. Rossiter R A *Astrophys. J.* **60** 15 (1924)
238. McLaughlin D B *Astrophys. J.* **60** 22 (1924)
239. Winn J N et al. *Astrophys. J. Lett.* **718** L145 (2010)
240. Southworth J "EPCat: catalogue of the physical properties of transiting planetary systems", http://www.astro.keele.ac.uk/jkt/tepcat/tepcat.html
241. Triaud A H M J *Astron. Astrophys.* **534** L6 (2011)
242. Brothwell R D et al. *Mon. Not. R. Astron. Soc.* **440** 3392 (2014)
243. Di Gloria E, Snellen I A G, Albrecht S *Astron. Astrophys.* **580** A84 (2015)
244. Cegla H M et al. *Astron. Astrophys.* **588** A127 (2016)
245. Boué G et al. *Astron. Astrophys.* **550** A53 (2013)
246. Hirano T et al. *Astrophys. J.* **742** 69 (2011)
247. Brown D J A et al. *Mon. Not. R. Astron. Soc.* **464** 810 (2017)
248. Charbonneau D, Jha S, Noyes R W *Astrophys. J.* **507** L153 (1998)
249. Martins J H C et al. *Astron. Astrophys.* **576** A134 (2015)
250. Line M R, Parmentier V *Astrophys. J.* **820** 78 (2016)
251. Wyttenbach A et al. *Astron. Astrophys.* **577** A62 (2015)
252. Temple L Y et al. *Mon. Not. R. Astron. Soc.* **471** 2743 (2017)

253. Dravins D et al., in *18th Cambridge Workshop on Cool Stars, Stellar Systems, and the Sun, Proc. of the Conf., Lowell Observatory, 8–14 June, 2014* (Eds G van Belle , H C Harris) (Flagstaff, AZ: Lowell Observatory, 2015) p. 853
254. Dravins D et al. *Astron. Astrophys.* **605** A90 (2017)
255. Dravins D et al. *Astron. Astrophys.* **605** A91 (2017)
256. Freytag B et al. *J. Comput. Phys.* **231** 919 (2012)
257. Abt H A, Moyd K I *Astrophys. J.* **182** 809 (1973)
258. Abt H A, Tan H, Zhou H *Astrophys. J.* **487** 365 (1997)
259. Klochkova V G et al. *Astron. Astrophys.* **345** 905 (1999)
260. Morales F Y et al. *Astrophys. J. Lett.* **730** L29 (2011)
261. Montgomery S L, Welsh B Y *Publ. Astron. Soc. Pac.* **124** 1042 (2012)
262. Welsh B Y, Montgomery S *Publ. Astron. Soc. Pac.* **125** 759 (2013)
263. Panchuk V E, Klochkova V G *Priroda* (3) 47 (2017)
264. Strassmeier K G et al. *Astron. Nachrich.* **336** 324 (2015)
265. Pepe F et al. *Astron. Nachrich.* **335** 8 (2014)
266. Magain P *Astron. Astrophys.* **297** 686 (1995)
267. Piskunov N et al. "User requirements and technical specifications for the VLC of the CES", ESO Nov. 12 (1997)
268. Panchuk V E *Byull. Spets. Astrofiz. Observ.* **44** 127 (1997)
269. Klochkova V, Panchuk V, Zhao G *Astrophys. Rep. Publ. Beijing Astron. Obs.* **34** 97 (1999)
270. Panchuk V E et al., in *Stars: From Collapse to Collapse, Proc. of a Conf., Nizhny Arkhyz, Russia 3–7 October 2016* (Astron. Soc. Pacific Conf., Vol. 510, Eds Yu Yu Balega et al.) (San Francisco, CA: Astronomical Society of the Pacific, 2017) p. 566
271. Panchuk V E *Izv. Vyssh. Uchebn. Zaved. Priborostroenie* **60** 753 (2017)
272. Selsis F et al. *Astron. Astrophys.* **476** 1373 (2007)
273. Shectman S A, Johns M *Proc. SPIE* **4837** 910 (2003)
274. Follert R et al. *Proc. SPIE* **9147** 914719 (2014)
275. Piskunov N, in *Stars: From Collapse to Collapse, Proc. of a Conf., Nizhny Arkhyz, Russia 3–7 October 2016* (Astron. Soc. Pacific Conf., Vol. 510, Eds Yu Yu Balega et al.) (San Francisco, CA: Astronomical Society of the Pacific, 2017) p. 514
276. Bean J L et al. *Astrophys. J.* **713** 410 (2010)
277. Otarola A C, Querel R, Kerber F, in *Comprehensive Characterization of Astronomical Sites, Conf., October 4–10, 2010, Kislovodsk, Russia*; arXiv:1103.3025
278. Otárola A et al. *Publ. Astron. Soc. Pac.* **122** 470 (2010)
279. Seifahrt A et al. *Astron. Astrophys.* **524** A11 (2010)
280. Borucki W J et al., in *Planets Beyond the Solar System and the Next Generation of Space Missions. Proc. of a Workshop, Baltimore, MD, October 16–18, 1996* (Astron. Soc. Pacific Conf., Vol. 119, Ed. D Soderblom) (San Francisco, CA: Astronomical Society of the Pacific, 1997) p. 153
281. Reynolds R O et al. *Proc. SPIE* **5170** 283 (2003)
282. Shefov N N, Semenov A I, Khomich V Yu *Izluchenie Verkhnei Atmosfery — Indikator ee Struktgury i Dinamiki* (Emission of the Upper Atmosphere as the Indicator of Its Structure and Dynamics) (Moscow: GEOS, 2006)
283. Hunter T R, Ramsey L W *Publ. Astron. Soc. Pac.* **104** 1244 (1992)
284. Spronck J F P, Schwab C, Fischer D A *Proc. SPIE* **7735** 77350W (2010)
285. Leon-Saval S G et al. *Opt. Lett.* **30** 2545 (2005)
286. Ghasempour A et al. *Proc. SPIE* **8450** 845045 (2012)
287. Panchuk V E, Yushkin M V, Yakopov M V *Astrophys. Bull.* **66** 355 (2011); *Astrofiz. Byull.* **66** 382 (2011)
288. Vogt S S et al. *Publ. Astron. Soc. Pac.* **126** 359 (2014)
289. Szentgyorgyi A H et al. *Proc. SPIE* **3355** 242 (1998)
290. Gorskii S M, Lebedev V P *Bull. Crimean Astrophys. Obs.* **57** 187 (1977); *Izv. Krymsk. Astrofiz. Observ.* **57** 228 (1997)
291. Gorskii S M, Kozhevatov I E, Lebedev V P *Sov. Astron.* **23** 332 (1979); *Astron. Zh.* **56** 590 (1979)
292. Kozhevatov I E, in *Issledovaniya po Magnetizmu, Aeronomii i Fizike Solntsa* (Studies on Geomagnetism, Aeronomy, and Solar Physics) (64) 42 (1983)
293. Erskine D J, Ge J, in *Imaging the Universe in Three Dimensions. Proc. of the ASP Conf.* (Astron. Soc. Pacific Conf., Vol. 195, Eds W van Breugel, J Bland-Hawthorn) (San Francisco, CA: Astronomical Society of the Pacific, 2000) p. 501
294. Ge J *Astrophys. J.* **571** L165 (2002)
295. Erskine D J *Publ. Astron. Soc. Pac.* **115** 255 (2003)
296. Ge J et al. *Astrophys. J.* **648** 683 (2006)
297. Mahadevan S et al. *Proc. SPIE* **5170** 184 (2003)
298. Ge J et al. *Bull. Am. Astron. Soc.* **36** 1407 (2004)
299. Barden S C *Proc. SPIE* **8446** 844639 (2012)
300. Charbonneau D et al. *Astrophys. J.* **568** 377 (2002)
301. Vidal-Madjar A et al. *Astrophys. J.* **604** L69 (2004)
302. Linsky J L et al. *Astrophys. J.* **717** 1291 (2010)
303. Sing D K et al. *Mon. Not. R. Astron. Soc.* **416** 1443 (2011)
304. Swain M R, Vasisht G, Tinetti G *Nature* **452** 329 (2008)
305. Tinetti G et al. *Astrophys. J.* **712** L139 (2010)
306. Gibson N P, Pont F, Aigrain S *Mon. Not. R. Astron. Soc.* **411** 2199 (2011)
307. Crouzet N et al. *Astrophys. J.* **761** 7 (2012)
308. Gibson N P et al. *Mon. Not. R. Astron. Soc.* **419** 2683 (2012)
309. Gibson N P et al. *Mon. Not. R. Astron. Soc.* **422** 753 (2012)
310. Pont F et al. *Mon. Not. R. Astron. Soc.* **385** 109 (2008)
311. Deming D et al. *Astrophys. J.* **774** 95 (2013)
312. Huitson C M et al. *Mon. Not. R. Astron. Soc.* **434** 3252 (2013)
313. Hubeny I, Burrows A, Sudarsky D *Astrophys. J.* **594** 1011 (2003)
314. Sing D K et al. *Mon. Not. R. Astron. Soc.* **436** 2956 (2013)
315. Wakeford H R et al. *Mon. Not. R. Astron. Soc.* **435** 3481 (2013)
316. Nikolov N et al. *Mon. Not. R. Astron. Soc.* **437** 46 (2014)
317. Ehrenreich D et al. *Astron. Astrophys.* **570** A89 (2014)
318. Werner M et al. *Astrophys. J. Suppl.* **154** 1 (2004)
319. Bourrier V et al. *Astron. Astrophys.* **597** A26 (2017)
320. Seager S, Sasselov D D *Astrophys. J.* **537** 916 (2000)
321. Aronson E, Piskunov N *Astrophys. J.* **155** 208 (2018)
322. Sachkov M, Shustov B, Gómez de Castro A I *Adv. Space Res.* **53** 990 (2014)
323. Sachkov M et al. *Astron. Nachrich.* **335** 46 (2014)
324. Sachkov M, Vlasenko O, in *40th COSPAR Scientific Assembly, 2–10 August 2014, Moscow, Russia* (Moscow: Lomonosov Moscow State Univ., 2014) E1.11-28-14
325. Panchuk V et al. *Astrophys. Space Sci.* **354** 163 (2014)
326. Reutlinger A et al. *Astrophys. Space Sci.* **335** 311 (2011)
327. Sachkov M et al. *Stars: From Collapse to Collapse, Proc. of a Conf., Nizhny Arkhyz, Russia 3–7 October 2016* (Astron. Soc. Pacific Conf., Vol. 510, Eds Yu Yu Balega et al.) (San Francisco, CA: Astronomical Society of the Pacific, 2017) p. 573
328. Shustov B et al. *Astrophys. Space Sci.* **335** 273 (2011)
329. Shustov B et al. *Astrophys. Space Sci.* **354** 155 (2014)
330. Shustov B et al. *Astrophys. Space Sci.* **363** 62 (2018)
331. Malkov O et al. *Astrophys. Space Sci.* **335** 323 (2011)
332. Boyarchuk A A et al. *Astron. Rep.* **60** 1 (2016); *Astron. Zh.* **93** 3 (2016)
333. Shematovich V, in *39th COSPAR Scientific Assembly, 14–22 July 2012, Mysore, India* (Mysore: Narayana Murthy Centre of Infosys Campus) p. 1773, C2.1-12-12
334. Lammer H et al. *Proc. IAU Symp.* **7** (S282) 525 (2012)
335. Fossati L et al. *Astrophys. J.* **720** 872 (2010)
336. France K et al. *Astrophys. J.* **712** 1277 (2010)
337. Knutson H A et al. *Astrophys. J.* **655** 564 (2007)
338. Shkolnik E et al. *Astrophys. J.* **676** 628 (2008)
339. Panchuk V, Sachkov M, Klochkova V *Proc. SPIE* **10702** 107022R (2018)
340. Panchuk V E, Sachkov M E, Klochkova V G *Vestn. Nauch. Proizv. Ob'ed. im. S A Lavochkina* (2) 42 (2018)
341. Klochkova V G, Panchuk V E, Sachkov M E, in *Sbornik Trudov Memorial'noi Konf. 2018 g. Pamyati Akademika A.A. Boyarchuka* (Proc. of the Memorial Conf. — 2018 Devoted to Acad. A A Boyarchuk) (Eds D V Bisikalo, D Z Vibe) (Moscow: Yanus-K, 2018) p. 394
342. Ioannisiani B K *Astrofiz. Issled. Spets. Astrofiz. Observ.* **3** 3 (1971)
343. Ioannisiani B K, Gambovskii G A, Konshin V M *Izv. Krymsk. Astrofiz. Observ.* **55** 208 (1976)
344. Sadovnichii V A, Cherepaschuk A M *Priroda* (3) 3 (2015)
345. Krugov V D *Soobsch. Spets. Astrofiz. Observ.* (56) 21 (1987)
346. Panchuk V E, Klochkova V G, in *Spetsial'naya Astrofizicheskaya Observatoriya Rossiiskoi Akademii Nauk. 50 Let* (Special Astrophysical Observatory of the Russian Academy of Sciences. 50 Years) (Nizhny Arkhyz: SAO, 2018) p. 46
347. Panchuk V E et al. *J. Opt. Technol.* **76** 87 (2009); *Opt. Zh.* **76** (2) 42 (2009)
348. Panchuk V et al. *Proc. SPIE* **9908** 99086Y (2016)

349. Panchuk V E et al., in *Stars*: *From Collapse to Collapse, Proc. of a Conf., Nizhny Arkhyz, Russia 3–7 October 2016* (Astron. Soc. Pacific Conf., Vol. 510, Eds Yu Yu Balega et al.) (San Francisco, CA: Astronomical Society of the Pacific, 2017) p. 562
350. Panchuk V E et al. *Izv. Vyssh. Uchebn. Zaved. Priborostroenie* **60** (1) 53 (2017)
351. Panchuk V E, Chuntonov G A, Naidenov I D *Astrophys. Bull.* **69** 339 (2014); *Astrofiz. Byull.* **69** 360 (2014)
352. Marov M Ya, Shematovich V I, Bisicalo D V *Space Sci. Rev.* **76** 1 (1996)
353. Kolesnichenko A V, Marov M Ya *Solar Syst. Res.* **40** 1 (2006); *Astron. Vestn.* **40** 3 (2006)
354. Shematovich V I, Marov M Ya *Phys. Usp.* **61** 217 (2018); *Usp. Fiz. Nauk* **188** 233 (2018)
355. Bisikalo D V et al. *Astrophys. J.* **869** 108 (2018)